Upper Miocene colluvial and alluvial fan deposits of the Modrová Mb.: A window to palaeogeography of the Považský Inovec Mts. (Western Carpathians)

Michal Šujan[1], Klement Fordinál[2], Katarína Šarinová[3], Samuel Rybár[1] & Ondrej Pelech[2]

[1] Department of Geology and Paleontology, Faculty of Natural Sciences, Comenius University in Bratislava, Ilkovičova 6, 842 15 Bratislava, Slovakia; miso@equis.sk
[2] State Geological Institute of Dionýz Štúr, Mlynská dolina 1, 817 04 Bratislava 11, Slovakia; klement.fordinal@geology.sk
[3] Department of Mineralogy and Petrology, Faculty of Natural Sciences, Comenius University in Bratislava, Ilkovičova 6, 842 15 Bratislava, Slovakia

AGEOS

Abstract: The study focuses on the upper Miocene colluvial to alluvial fan deposits of the Modrová Mb., which accumulated on the marginal blocks of the Považský Inovec Mts., transitional to surrounding depressions of the Danube Basin. These blocks are delimited tectonically according to the geophysical evidence, and the late Miocene normal faulting produced fault scarps causing rapid sediment supply. However, the supply of coarse clastics composed mostly of Mesozoic dolomites was of intensity sufficient only to fill the accommodation of the marginal blocks. The sediment input to the surrounding Danube Basin is on the both sides of the Považský Inovec Mts. not traceable, probably due to an overwhelming alluvial redistribution. Facies analysis of the Modrová Mb. implies an environment of colluvial fans with prevalence of cohesive debris flow deposition, associated with less frequent rockfall, grain flow and sheetwash processes on the western side of the mountains in the area of Modrová village. In contrary, the easterly situated area of Tesáre village exhibits dominance of debris flow deposition with more than one third of the succession deposited by channelized and unchannelized shallow traction currents, indicating sedimentary environment of an alluvial fan close to its transition to colluvial sediment-feeder system. Petrographical and geochemical study showed extremely low content of siliciclastic component in the colluvial deposits of the Modrová area. Dolomite clasts form a major part of the sediment and are covered by a coating of clay minerals. The coatings and sediment matrix contain iron oxides possibly derived by fersiallitic weathering and by oxidation of pyrite scattered within the matrix. Geochemistry of muddy layers in the Tesáre succession implies either cold or dry weathering conditions. However, weathering proxies are considered to be biased due to the rapid denudation in the colluvial to alluvial fan environment, since observed facies and published regional studies imply rather warm and humid climate. Several examples of simultaneous comparable depositional settings in the broader region imply, that these colluvial to alluvial fan successions could be related to a mild phase of regional tectonic activity at ~8 Ma.

Key words: facies analysis, Pannonian Basin System, late Miocene, palaeoenvironment, weathering, syntectonic deposition

1. INTRODUCTION

Achievement of a precise palaeogeographic reconstruction is typically complicated in terrestrial environments of active orogens, where frequent periods of erosion or non-deposition cause scarcity of depositional record. River terrace systems are widely used for palaeotopographic and surface uplift histories, but more elevated topographies commonly lack fluvial accumulations (Merritts et al., 1994). These areas might comprise planation surfaces more resistant to denudation in comparison to river terraces, which are, however, complicated for dating (Ruszkiczay-Rüdiger et al., 2011; Wagner et al., 2011).

Specific conditions of subaerial exposure and stable local erosional base in a hilly relief is favourable for accumulation of colluvial deposits, especially in the case of slopes predisposed by active faulting (e.g., Swan, 1988; Nelson, 1992). Colluvial fans or gravity flow-dominated alluvial fans are an example of such successions (Blikra & Nemec, 1998). Their areal distribution, facies and composition could point to palaeotopographic state and palaeoclimatic evolution of a specific area (Nemec & Kazanci, 1999; Sanders et al., 2018).

The Western Carpathians represent an Alpine orogenic belt with uplift tendencies evolving to the present times (Minár et al., 2011). Their neotectonic uplift history is complex and not yet described in detail (e.g., Danišík et al., 2004; Králiková et al., 2016; Kováč et al., 2017). This study focuses on the upper Miocene colluvial to alluvial fan successions of the Modrová Member, which was deposited on the marginal parts of the Považský Inovec Mts. The aim of the study is to investigate the palaeogeographic and palaeoenvironmental significance of the studied deposits, and especially to examine the role, which played the horst exposed on the margins of the Western Carpathians as a source of sediment supply and also as a barrier for drainage network during the late Miocene.

2. GEOLOGICAL SETTING

The Western Carpathians were formed to their present shape by the Alpine orogenesis during the Late Jurassic to recent times (Hók et al., 2014; Kováč et al., 2017; Plašienka et al., 2020). The framework of horsts and basins resulted from extension

Manuscript received 2020-10-14
Revised version accepted 2021-03-29

related to subduction processes in the forearc area during the Miocene (Kováč et al., 2018[a]). The extensional tectonics was followed by domatic uplift of the mountain chain during the neotectonic period, which is possibly related to the inversion of the Pannonian Basin System (PBS) starting at ~6 Ma (Horváth et al., 2006; Balázs et al., 2016; Šujan et al., 2021). The basin system borders with the Western Carpathians on their southern side (Fig. 1B).

The Považský Inovec Mts. (PI Mts.) locates on the western margin of exposed Western Carpathian massifs and is surrounded by the Blatné and Rišňovce depressions (sub-basins) of the Danube Basin (Fig. 1), which is the northernmost depocenter of PBS (Kováč, 2000). The oldest and structurally lowermost part of PI Mts. is represented by the pre-Alpine (Variscan) crystalline basement of the Tatric tectonic unit. In the central part of the mountain range, where the investigated area is located, the crystalline basement is composed of granitic and metamorphic rocks (Fig. 2). The Tatric crystalline basement rocks are overlain by the Permian to Upper Cretaceous (Cenomanian–Turonian) sedimentary cover succession, which is overridden Mesozoic nappes of Fatric and Hronic units with prevailing carbonate lithology (Ivanička et al., 2007, 2011, Prokešová et al., 2012, Havrila, 2011). The formations of the Hronic Unit are usually unconformably overlain by the Paleogene and Neogene sediments (Ivanička et al., 2011).

PI Mts. has undergone diverse exhumation which is documented by the zircon (ZFT) and apatite fission-track (AFT) data, as well as the sedimentary record and geological mapping. AFT data indicates that exhumation was gradual and lasted since the middle to late Eocene (approx. 40 Ma) in the southern part of PI Mts., to the early Miocene (~20 Ma) in the central part of the mountains up to the late middle Miocene (~13 Ma) in the northern part of the mountains (Kováč et al., 1994; Danišík et al., 2004; Králiková et al., 2016).

The Blatné and Rišňovce depressions started to be filled during the syn-rift stage of the PBS dated in the area from the early

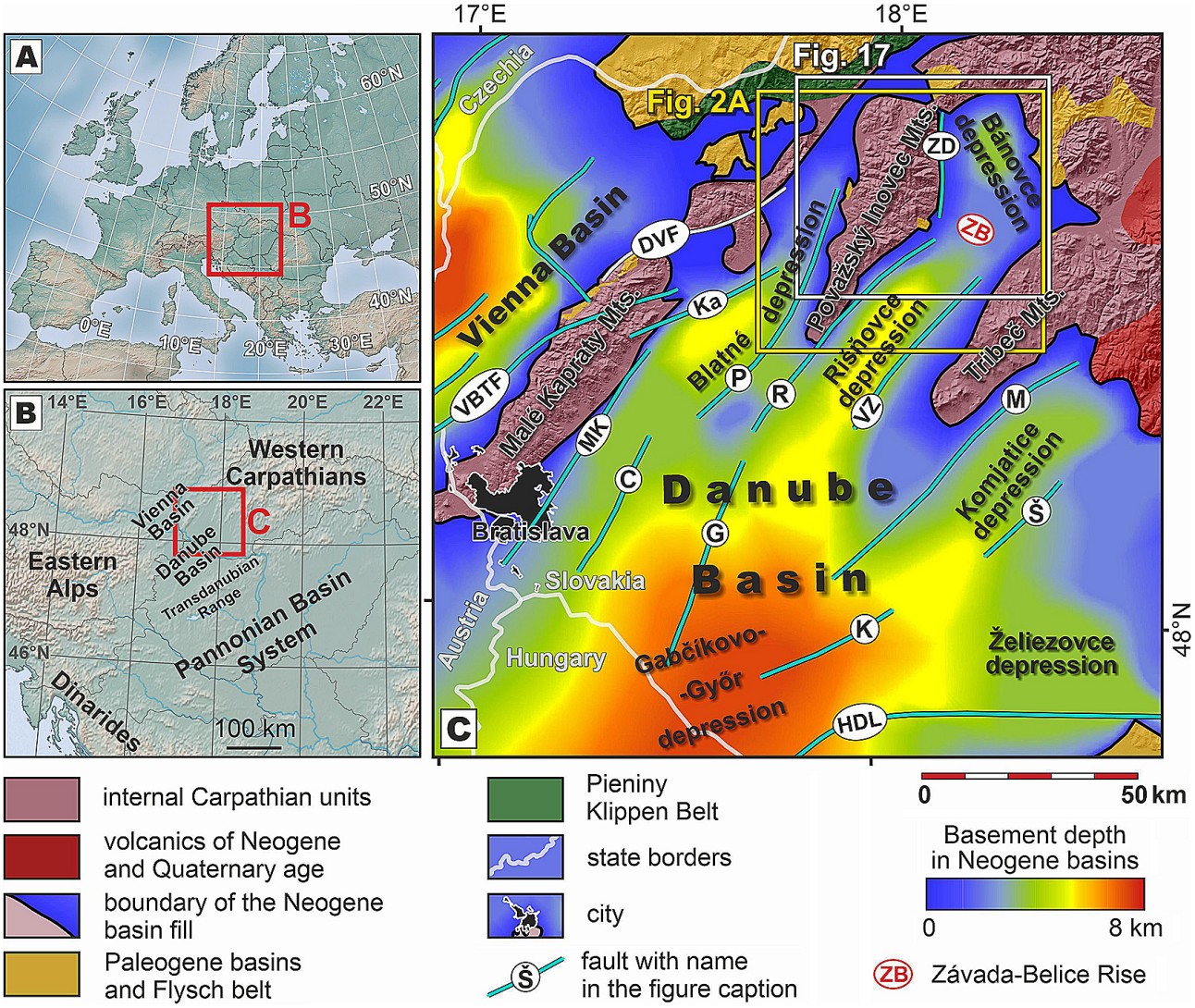

Fig. 1A: Location of the study area in Central Europe. B: Situation of the Danube Basin and western margin of the Western Carpathians. C: Detailed position of the study area in the Považský Inovec Mts. Location of major faults active during the latest Cenozoic from Bielik et al. (2002), Lenhardt et al. (2007), Beidinger & Decker (2011) and Klučiar et al. (2016). Fault names: C – Cífer Fault, DVF – Dobrá Voda Fault, G – Galanta Fault, HDL – Hurbanovo-Diösjenő Fault, K – Kolárovo Fault, Ka – Kátlovce Fault, MK – Malé Karpaty Fault, P – Považie Fault, R – Ripňany Fault, Š – Šurany Fault, VBTF – Vienna Basin Transfer Fault, ZD – Závada-Dubodiel Fault.

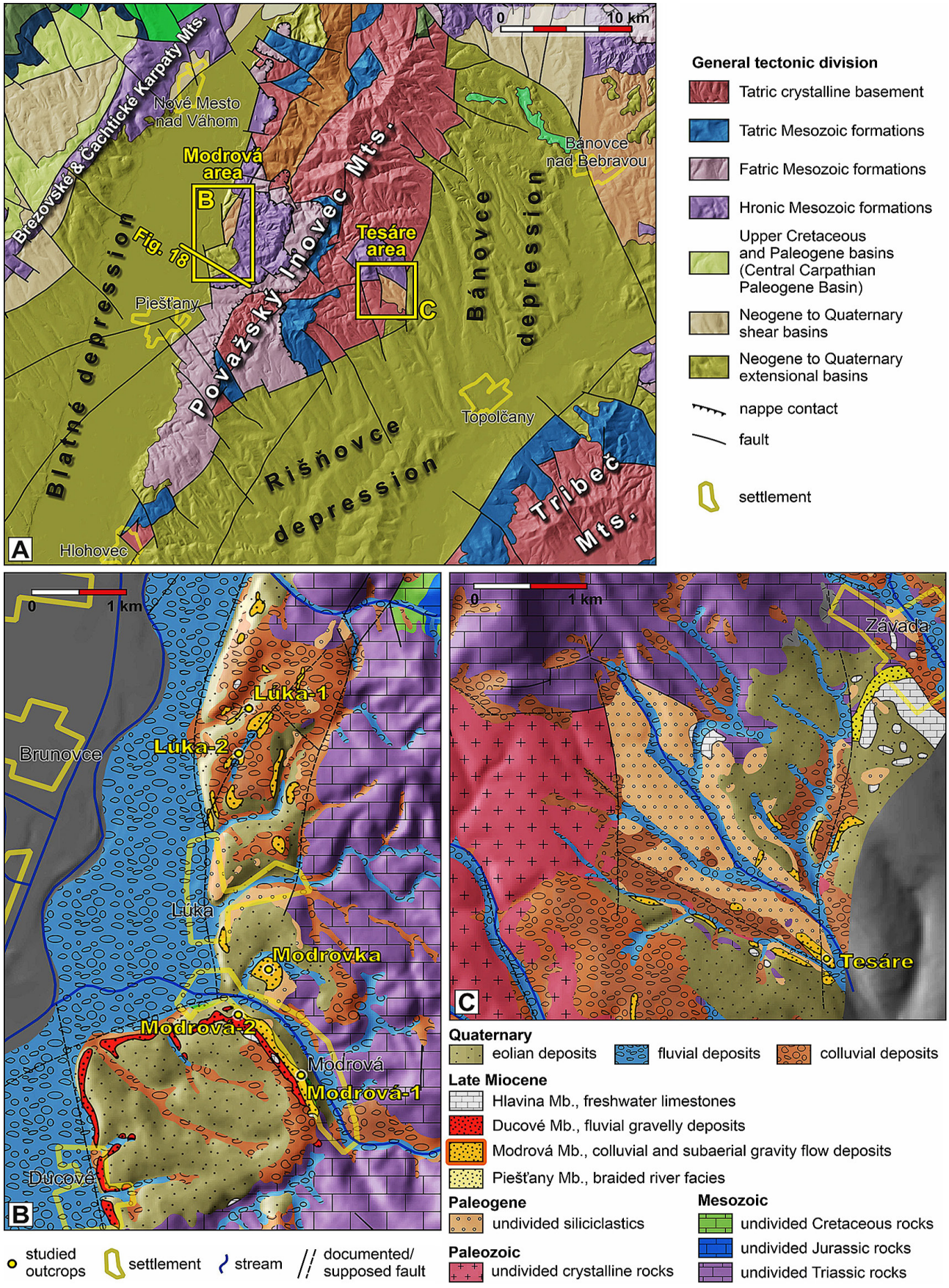

Fig. 2A: Generalized tectonic map of the studied part of the Považský Inovec Mts. and adjacent areas (modified from Ivanička et al., 2007). B: Geological map of the Modrová area with occurrence of the Modrová Mb. C: Geological map of the Tesáre area with occurrence of the Modrová Mb.

Badenian (Langhian, after ~15.2 Ma). The last rifting phase took place at ~11.6–9.5 Ma and the area experienced post-rift conditions after its cessation during the following period of ~9.5–6.0 Ma (Šujan et al., 2021). Some parts of the mountains were covered by the alluvial deposits of the Volkovce Fm. due to the overall base level rise (Šujan et al., 2017). However, analysis of the Volkovce Fm. alluvial sequence showed negligible input of clastic material directly from the mountain horst, because the gravelly Piešťany Mb. (Fig. 3) contains dominantly quartz and quartzite material indicating distant source located probably in the Central Western Carpathians (Šujan et al., 2017).

Following basin inversion after ~6 Ma led to interruption of the Volkovce Fm. deposition and to denudation. Nevertheless, the authigenic $^{10}Be/^{9}Be$ dating from the southern parts of the mountains near Hlohovec with ages around 6.5 Ma imply that only few tens of meters of upper Miocene sediment were eroded there (Šujan et al., 2016). More significant surface uplift appeared until the Early Pleistocene, as evidenced by formation of river terraces on the foothills of the mountains (Šarinová & Maglay, 2002; Šujan et al., 2016), by more pronounced fault activity and speleogenesis in the region (Putiška et al., 2014; Brixová et al., 2018[a,b]; Lačný et al., 2019; 2020; Kušnirák et al., 2020), as well as by increase of crystalline rocks supply from the mountains to the basin fill (Šujan et al., 2018).

The studied deposits of the Modrová Mb. are present in marginal parts of the Považský Inovec Mts. Detailed geological mapping revealed a lateral transition between the Modrová Mb. beds and freshwater limestones of the Hlavina Mb. (Fordinál in Ivanička et al., 2007), which have been dated to ~8 Ma by rodent biostratigraphy (Fig 3) (Kováč et al., 2011[a]). Hence, the Modrová Mb. accumulated synchronously with the Volkovce Fm. The Ducové Mb. is probably another lateral equivalent of the Volkovce Fm. on the foothills of the Považský Inovec Mts. However, lack of outcrops hampers identification of its detailed stratigraphic position and relations to other lithostratigraphic units. It is worth to mention that the Modrová Mb. is not yet a formally defined lithostratigraphic unit.

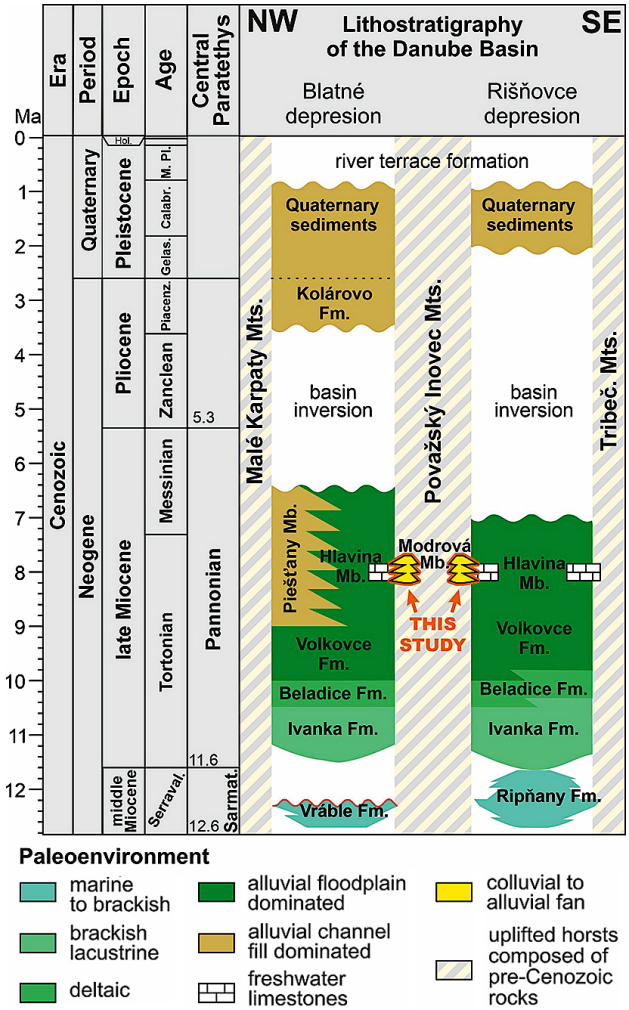

Fig. 3: Lithostratigraphic scheme of the upper Miocene deposits of the studied area according to Šujan et al. (2021). Palaeoenvironment is modified according to Fordinál & Elečko (2000), Vass (2002), Rybár et al. (2016), Sztanó et al. (2016) and Šujan et al. (2016). Timing of Central Paratethys stage boundaries according to Vasiliev et al. (2010) and Kováč et al. (2018[b]).

3. METHODS

3.1 Sedimentology and granulometry

The facies were described standardly according to the grain size, structure and texture, geometry and size of the strata and visualized in sedimentological logs. Depositional processes were interpreted based on observed association of the facies. The studied deposits exhibit various degree of lithification, what affected the level on which the outcrops could be cleaned and thus the precision of facies recognition. Palaeocurrent orientation measurement was possible in the case of the Tesáre outcrop, where cross-stratified beds were present. Six gravelly samples from the Modrová-2 locality and five samples from the Tesáre locality were analysed for granulometry using sieving. Lithified samples were cross-cut and scanned to observe the internal structure.

3.2 Geochemistry

Fine fraction (< 0.064 mm) from eight granulometric samples underwent analysis of major and trace elements. This comprise matrix of four gravelly samples from the Modrová-2 locality (Mod-3, Mod-4, Mod-5 and Mod-6) and another four samples from sandy strata of the Tesáre locality (Tes-1, Tes-2, Tes-3 and Tes-4), separated from the coarser fractions by sedimentation in a water column. The samples were pulverised, dissolved by Lithium Borate Fusion and analysed by ICP-ES (major oxides) ICP-MS (trace elements) in Bureau Veritas mineral laboratories (Canada, Vancouver). Content of C and S was analysed by LECO Carbon-Sulphur analyser.

Thin sections of lithified gravel from the Lúka-2 locality were prepared in order to investigate composition of its cement, which was the subject of microprobe analysis by Cameca SX 100 (State Geological Institute of Dionýz Štúr). Minerals were measured using WDS analysis with accelerating voltage 15 keV, probe current 10 nA.

4. RESULTS

4.1 Modrová area outcrops – colluvial fan facies association

4.1.1 Description

The Modrová area includes several outcrops on the western margin of PI Mts. (coordinates in Suppl. Table 1). The Modrová Mb. is exposed in stream gorges, for example on the Lúka-1 locality (Fig. 4), where it constitutes ill-sorted chaotic gravel with angular to sub-angular clasts composed of dolomite and sandstone. Another example of natural exposure could be observed on the Modrová-1 site (Fig. 5), where dolomitic gravel with angular clasts forms faintly bedded bodies on a cliff.

Fig. 5: Natural exposure of ill-sorted angular gravel with faint bedding on the Modrová-1 locality. Facies are not interpreted due to small exposure. See Fig. 2B for location.

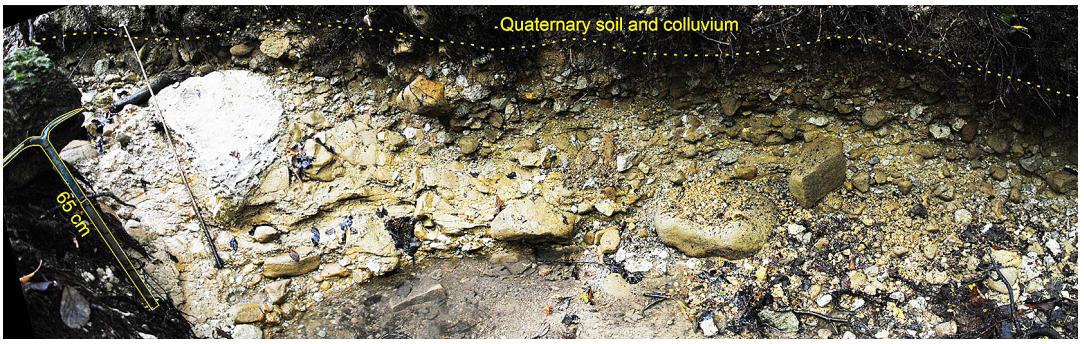

Fig. 4: Example of the Modrová Mb. exposure in a stream gorge on the Lúka-1 locality, which comprise chaotic ill-sorted gravel of sandstone and dolomite. Facies are not interpreted due to small exposure. See Fig. 2B for location.

Tab. 1: Description and interpretation of the lithofacies observed on the Modrová Mb. outcrops.

Code	Lithofacies description	Lithofacies geometry	Depositional process	Facies association
Gm	matrix-supported angular gravel, massive, ill-sorted, large clasts occasionally oriented parallel to the base, matrix mostly sandy mud, less muddy sand, ø 0.4–10 cm	laterally extensive as well as narrow lenticular bodies 20–120 cm thick, com-monly amalgamated, non-erosive base, boundaries poorly defined, inclined up to 20°	cohesive subaerial debris flow (Nemec & Steel, 1984; Mulder & Alexander, 2001)	colluvial as well as alluvial fan
Sgm	muddy sand with presence of floating granules and pebbles, massive	laterally extensive bodies 10–30 cm thick, sharply bounded	cohesive subaerial debris flow (Nemec & Steel, 1984; Mulder & Alexander, 2001)	colluvial fan
Gkr	clast-supported angular gravel, massive to normally-graded, ill-sorted, matrix muddy sand to sandy mud, ø 0.4–6 cm	narrow lenticular, less laterally extensive bodies 20–60 cm thick, commonly deposit-ed above erosional base, inclined up to 20°	rockfall (Blikra & Nemec, 1998)	colluvial fan
Gkg	clast-supported angular gravel, massive- or reverse-graded, poorly- to moderately-sorted, matrix is absent or present in low amount, ø 0.4–4 cm	laterally extensive as well as narrow lenticular bodies few centimeters to 35 cm thick, commonly deposited above erosional base, inclined up to 20°	subaerial grainflow (Lowe, 1976; Nemec & Steel, 1984; Mulder & Alexander, 2001)	colluvial fan
Gkh	sandy angular gravel, faintly horizontally bedded, moderately-sorted, matrix composed of muddy sand	amalgamated laterally extensive bodies	sheetflow – shallow poorly confined traction current redistributing colluvial sediment on a short distance (Blikra & Nemec, 1998)	colluvial as well as alluvial fan
Gp	angular gravel forming faint planar cross-stratification, ill- to moderately-sorted, matrix muddy sand	laterally extensive bodies 20–50 cm thick, with sharp erosional base and top	channelized traction current, deposition on a shallow bar (Bridge & Lunt, 2006; Reesink, 2018)	alluvial fan
Gsi	angular gravel alternating with laminated muddy sand, moderately-sorted, forming inclined layers or lenses within tabular bodies	laterally extensive bodies 15–40 cm thick, sharply bounded	channelized traction current with periodical variation in the stream competence, deposition on a shallow bar	alluvial fan
Sgl	muddy sand with granules, faintly- to well-laminated	laterally extensive bodies 5–25 cm thick, sharply bounded	sheetflow – shallow poorly confined traction current (Blikra & Nemec, 1998)	alluvial fan
Sl	muddy sand to sandy mud, faintly- to well-laminated	tabular bodies 2–15 cm thick, sharply bounded	shallow and slow traction current, silty ripples migrating in low sedimentation rate (Yawar & Schieber, 2017)	alluvial fan

Fig. 6: Sedimentological log and photo documentation of the outcrop in abandoned quarry in the Modrová-2 site with location of samples analysed for granulometry and geochemistry. The nature of the outcrop allowed cleaning and recognition of four lithofacies. Degree numbers on B indicate strike orientation of the outcrop wall. For codes of lithofacies see Tab. 1 and for location see Fig. 2B.

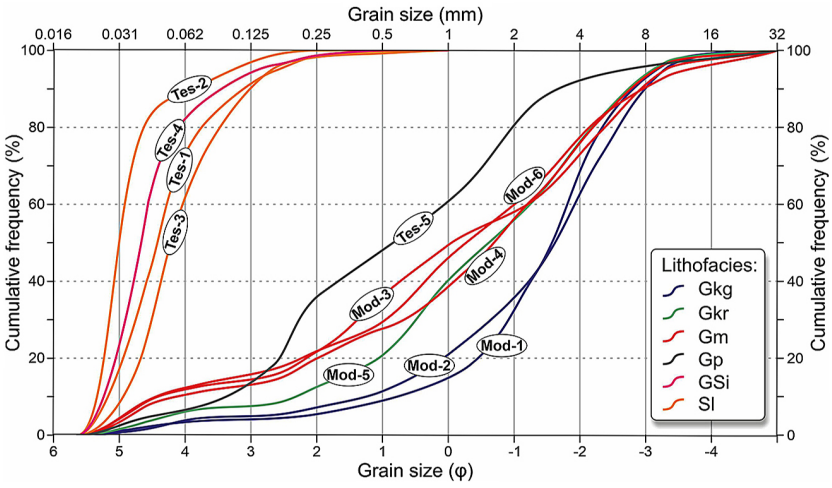

Fig. 7: Cumulative frequency of grain size fraction of the samples taken from localities of Modrová (Mod) and Tesáre (Tes).

Unlike the mentioned localities, the Modrová-2 locality comprises an abandoned quarry exposing >10 m thick loose to lithified dolomitic gravel, what allowed cleaning and detailed facies observations (Fig. 6). The outcrop consists of three lithofacies. The most common are laterally continuous as well as narrow lenticular bodies of matrix-supported angular ill-sorted chaotic gravel (code Gm), which comprise 66.4 % of the sedimentological log (Fig. 6C–G). Matrix is composed of reddish sandy mud. Some of the bodies exhibit matrix- to clast-supported structure. The Gm lithofacies are commonly amalgamated and their base is non-erosive and poorly defined. Thickness of an individual unit reaches 20–120 cm, with an average of 45 cm. Cumulative grain size distribution of three samples on Fig. 7 illustrates the low level of sorting of the lithofacies Gm, as well as relatively high content of fine fraction below 0.062 mm reaching 12 % of a sample weight. The sorting coefficient according to Folk & Ward (1957) reaches values of 2.41–2.65 implying very poor sorting.

The second most abundant lithofacies (22.8 % of the log) comprise clast-supported angular ill-sorted gravel (code Gkr), which is massive or normally graded (Fig. 6D, E, G). Matrix is composed of reddish muddy sand to sandy mud. The lithofacies form mostly narrow lenticular bodies with erosive concave base (Fig. 6D), laterally continuous bodies are less common. The erosional origin of boundaries is interpreted based on their irregular shape, truncation of the below lying facies, sharp transition and dip of a boundary commonly exceeding 45°. Thickness attains 20–60 cm with an average value of 38 cm. Grain size distribution of one analysed sample indicates that sorting of Gkr is with the value of 2.08 according to Folk & Ward (1957) poor to very poor, hence comparable to the lithofacies Gm, however, consisting only half of the fraction below 0.062 mm (<7 %) (Fig. 7).

The lowest abundance of 10.8 % of the sedimentological log attains clast-supported poorly- to moderately-sorted, massive- to reverse-graded gravel with low content or absence of matrix (Gkg, Fig. 6C, D). The lithofacies form 5–35 cm thick (12 cm in average) laterally continuous as well as narrow lenticular bodies, mostly with poorly defined base and its erosional nature is seldom. The cumulative frequency of grain size of two analysed samples show poor to moderate sorting with values of 1.14 and 1.28 (Folk & Ward, 1957), differing to the previously mentioned facies Gm and Gkr. Major fraction is composed of clasts in the range of 1–10 mm (Fig. 7). The fine fraction below 0.062 mm attains <4 % of a sample weight.

The attitude of lithofacies on the Modrová-2 locality is apparently subhorizontal, however, the cleaned vertical section does not allow precise determination of their lateral correlation. Moreover, it exposes only 2D view on the stratal boundaries. Nevertheless, other exposures clearly show notable inclination of the strata. The Modrovka locality provides a good example

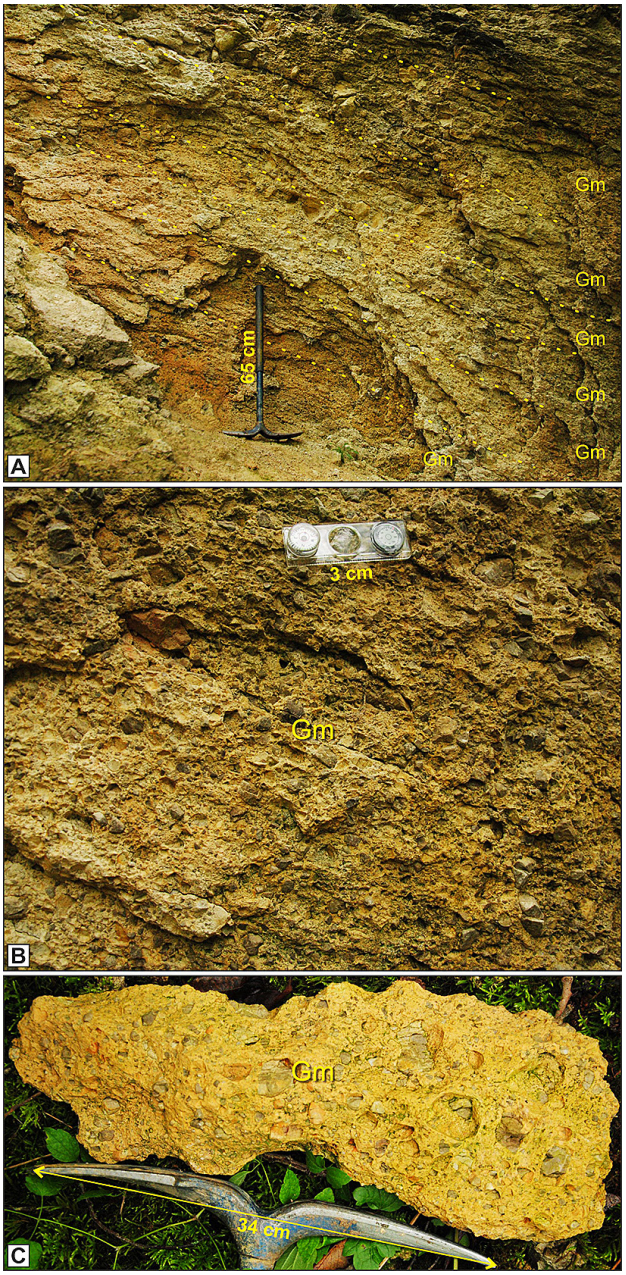

Fig. 8A,B: Example of the exposure of the Modrová Mb. with inclined bedding on the Modrovka locality. C: The matrix-supported rock is significantly lithified.

with inclination of massive matrix-supported gravel beds reaching ~25° and dip direction of 250° (Fig. 8). The gravel is significantly lithified (Fig. 8C).

Another outcrop showing dip of bedding was documented on the Lúka-2 locality (Fig. 9). Major portion of the section is composed of matrix-supported chaotic ill-sorted angular gravel (Gm). Ill-sorted massive angular clast-supported gravel is less common (Gkr). This lithofacies contain 1–3 cm thick horizons with increased sorting and lack of matrix (Fig. 9C,D). Upper part of the outcrop consists of faintly horizontally-bedded moderately-sorted clast-supported angular gravel (Gkh).

The appearance of lithified angular conglomerates of the lithofacies Gkr is illustrated by Fig. 10A. A reader can observe obvious visual difference of the Modrová Mb. conglomerate from rounded and moderately-sorted conglomerate of the Ducové Mb. on Fig. 10B, as well as from the well-sorted conglomerates with well-rounded clasts of the Paleogene Borové Fm. (Fig. 10C) present in the Modrová area (Fig. 2B).

4.1.2 Interpretation

The observations and interpretations of the facies are included in Table. 1. The deposits of lithofacies named as Gm are considered

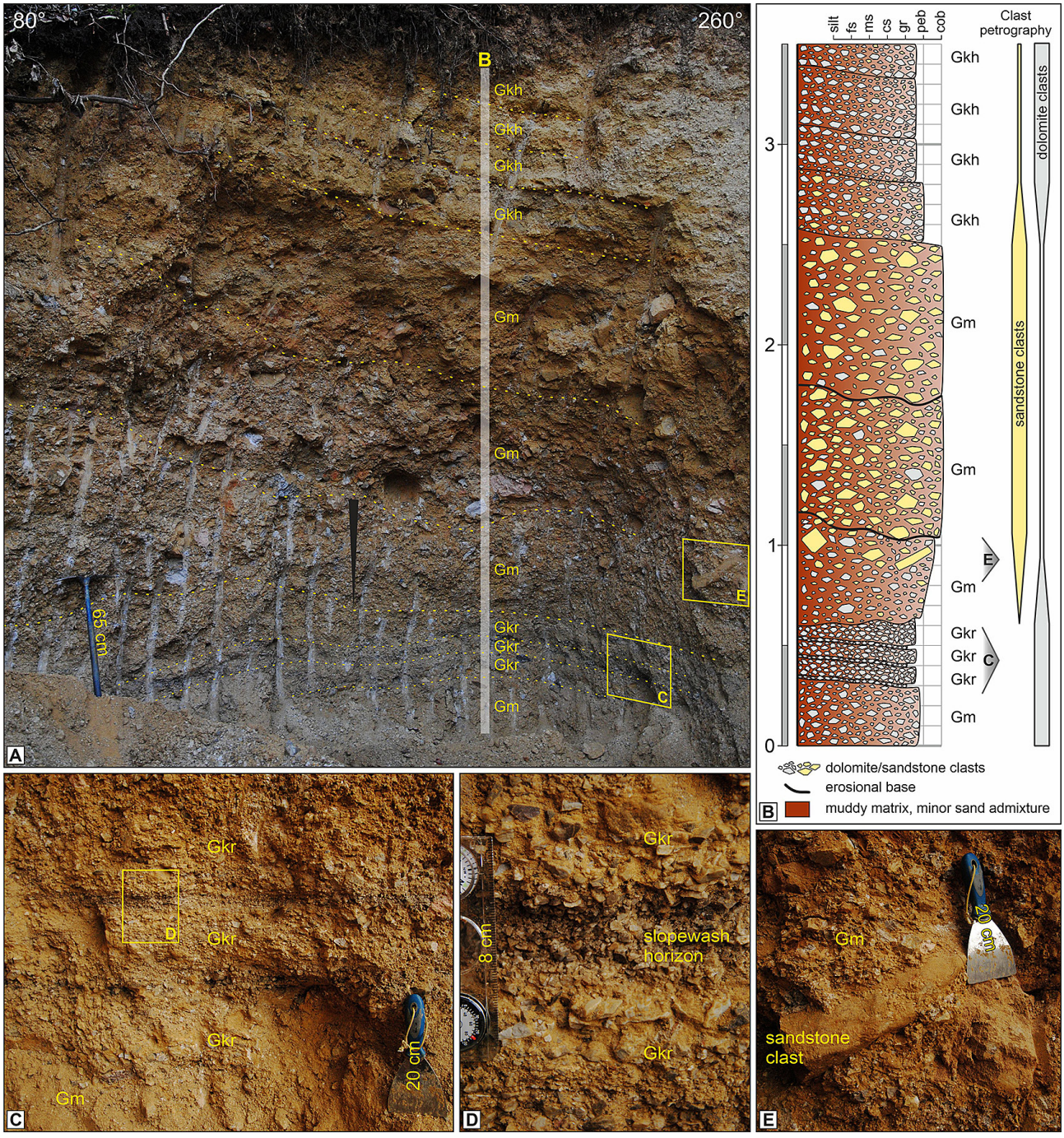

Fig. 9: Photo documentation and sedimentological log of the Lúka-2 locality. Degree numbers on B indicate strike orientation of the outcrop wall. For codes of lithofacies see Tab. 1 and for location see Fig. 2B.

to be formed by cohesive subaerial debris flows with moderately high viscosity (Nemec & Steel, 1984; Blikra & Nemec, 1998; Mulder & Alexander, 2001). Their deposition is characteristic by a lack of erosion on their base, in agreement with observed poorly defined boundaries. Fine-grained fraction of matrix reaching up to 12 % of a unit mass served as a source of cohesion and viscous behaviour of a flow. The nature of the flow causes linear movement and prevents sorting, what leads to overall chaotic texture (Costa, 1988; Iverson, 1997).

Lithofacies Gkr exhibits common normal grading with largest pebbles or cobbles on the base of a unit, indicating that clasts were freely segregated during their rolling in a rockfall transport mechanism (Blikra & Nemec, 1998). Locally increased content of matrix might be caused by coeval slope wash of muddy Gm lithofacies (Nemec & Kazanci, 1999).

The moderate to good sorting of Gkg gravel and low content of matrix, their relative thin bedded appearance and occasional reverse grading indicate that collisional stresses of gravel clasts were responsible for transport until frictional freezing of a grain flow (Lowe, 1976; Nemec & Steel, 1984; Nemec, 1990; Mulder & Alexander, 2001). Despite the depositional process comprise linear flow, dissipative stress and kinematic sorting leads to reverse grading of a grain flow if the flow reaches sufficient thickness (Bagnold, 1954; Sallenger, 1979; Legros, 2002).

Facies Gkh consisting of faintly horizontally-bedded clast-supported gravel indicates deposition of an unconfined traction current, which could be attributed to the sheetflow processes (Blikra & Nemec, 1998). Despite the facies was observed only on the Lúka-2 locality of the Modrová area, it reached >1 m of total thickness there.

The described depositional processes allow to classify the studied successions as a facies association of colluvial fans. The common presence of erosional base below rockfall and grain flow deposits imply that erosion preceded deposition in those cases. However, Gkg and Gkr facies represent highly sediment-concentrated gravity flows, hence the erosion on the base of such flow is negligible and the flows mostly cover the pre-existing topography (e.g., Nemec & Steel, 1984). Colluvial fans are commonly the most proximal depositional forms sourcing more distally situated alluvial fan environments, where depositional processes related to water traction current prevail (e.g., Blair & McPherson, 1994; Longhitano et al., 2015). Highly sediment-concentrated gravity flows accumulate positive forms with irregular shape, which tend to confine water runoff into gullies (Valentin et al., 2005). It is possible to assume that water runoff might cause gully erosion on the surface of a colluvial fan, but the flow was only erosional in this zone and formed accumulations in a more distal position, which is not preserved within the studied sections. The relief incised by gullies would be then covered by rockfall and grain flow deposits, similarly, as documented by Nemec & Kazanci (1999).

Evidence for a wash out of matrix from rockfall deposit by slope wash was observed on the Lúka-2 site (Fig. 9D). The episodic effect of a slope wash can be attributed to variation in depositional processes on the Modrová-2 locality (de Haas et al., 2014). When active, the slope wash would induce washing out of fine-grained fraction from intergranular space of debris flow deposits. The loss of matrix would cause slope instability and initiates redeposition of material by rockfall and grain flow, which cover the erosional surface formed by slope wash.

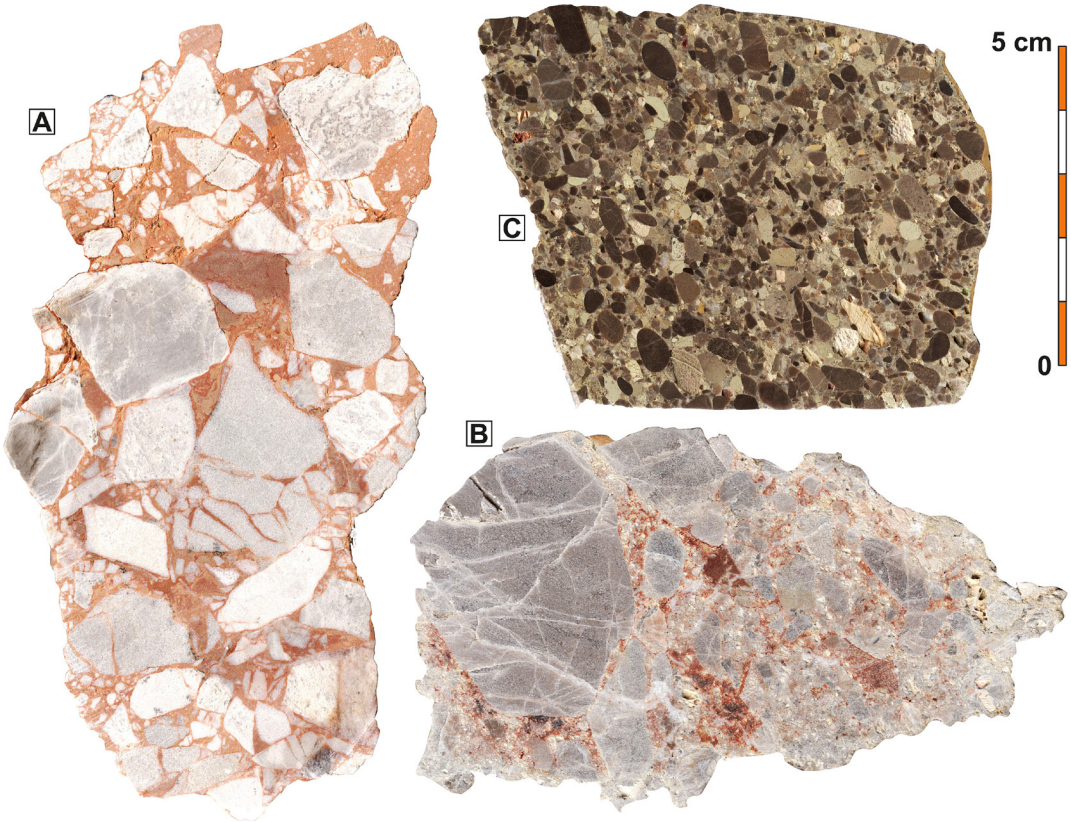

Fig. 10: Cross-cut lithified rock examples. A: Modrová Mb. conglomerate, Modrová-2 locality (Fig. 2B); B: Ducové Mb. conglomerate sampled in the vicinity of Ducové village (Fig. 2B); C: Paleogene conglomerate from the Modrová area. Note the differences in clast roundness.

Although the high observed inclination of beds reaching ~25° is considered as primary and resulting from high sediment supply in a colluvial environment, contribution of effects of preexisting topography and post-depositional tilting on the primary geometry couldn't be excluded.

4.2 Tesáre area outcrop – alluvial fan facies association

4.2.1 Description

Lack of more suitable outcrops on the eastern margin of PI Mts. allowed to study the Modrová Mb. only on the outcrop near Tesáre (Suppl. Table 1). The strata are exposed in an abandoned quarry with the wall reaching height >6.5 m (Fig. 11). A fault zone separates the outcrop to two successions, which do not exhibit comparable depositional record, hence the offset attains more than 6 m. Therefore, the depositional record is shown in two separate sedimentological logs (Fig. 12). The strata are oriented sub-horizontally in contrary to the settings observed in the Modrová area.

The first group of facies were observed also in the Modrová area. The most frequent facies, attaining 31.8 % of the strata thickness, comprise again ill-sorted chaotic matrix-supported gravel (Gm). However, the matrix composition varies from sandy mud up to muddy sand. Sharp erosive base is much more common in comparison to the Modrová area (Fig. 12E–G), marked mainly by truncation of below lying units. Thickness of a sedimentary unit ranges in 20–130 cm with an average of 54 cm. The second most common lithofacies consisting of clast-supported poorly- to moderately-sorted angular gravel with low content of matrix (Gkg) form 15.6 % of the studied section. The thickness of the individual strata reaches 4–60 cm with an average of 15 cm. The strata exhibit common reverse grading (Fig. 12D,E) and sometimes form lenticular bodies (Fig. 12E). Comparable abundance of 14.1 % attains lithofacies Gkh forming ca. 10 cm thick cycles of faintly horizontally bedded angular gravel with clast-supported texture. Nature of Gkh facies is well observable on Fig. 11B. Lithofacies Gkr with ill-sorted angular clast-supported gravel showing common normal grading forms 10.5 % of the studied succession (Fig. 12B).

Facies unrecognized in the Modrová area form 28 % of the Tesáre outcrop succession. The most common is faintly planar cross-stratified angular moderately-sorted gravel with sandy matrix (Gp, Fig. 12G). The lithofacies form laterally continuous units 15–64 cm thick and 11.3 % of the outcrop section. Cumulative grain size distribution of one sample of the lithofacies Gp on Fig. 7 depicts slightly better sorting, higher proportion of sand and lower content of mud comparing to lithofacies Gm and Gkr. Abundance of 5.9 % is reached by massive chaotic muddy sand with floating angular gravel clasts with thickness 7–20 cm (SGm, Fig. 12B). Relatively unusual is planar cross-stratified gravel with presence of lenses of muddy sand within the stratification (GSi; Fig. 12C, F). The gravel layers on foresets are commonly normally graded (Fig. 12C). Thickness of each unit varies up to 30 cm since it covers irregular erosive surface. The last observed lithofacies comprise laminated muddy sand to sandy mud, which form layers 2–10 cm thick (4.4 cm in average) (Sl, Fig. 12C,D). The lithofacies Sl is commonly eroded by the overlying unit, hence continuous layers are sparse. Grain-size distribution of the three analysed samples of Sl implies that the content of silt and clay reaches 60–95 % of a sample mass and the rest is formed mostly by fine-grained sand (Fig. 7). The sample Tes-4 was taken from the muddy sand lens of the

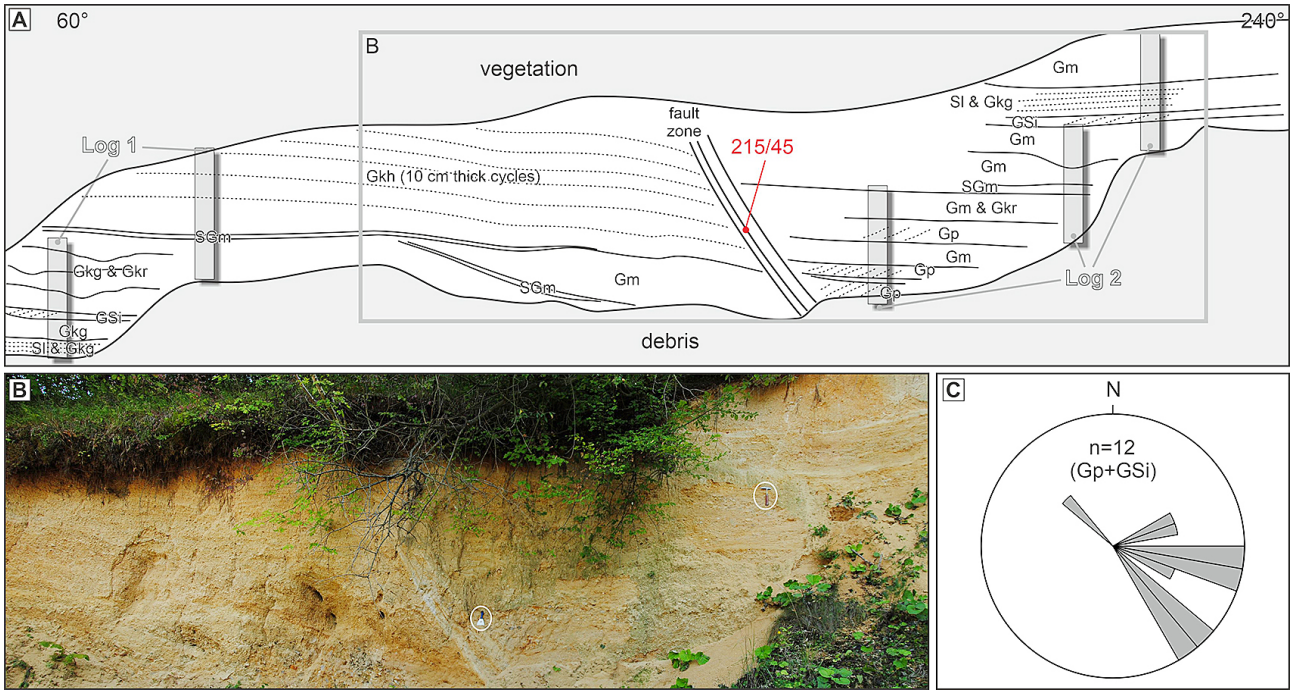

Fig. 11: General scheme of the Tesáre outcrop. Degree numbers on A indicate strike orientation of the outcrop wall. For codes of lithofacies see Tab. 1 and for location see Fig. 2B. C: Rose diagram of palaeocurrent measurements.

lithofacies GSi and exhibit comparable grain size composition to the Sl lithofacies. All mentioned samples show moderate to moderately well sorting (0.66–0.84), (Folk & Ward, 1957).

4.2.2 Interpretation

The depositional processes of the Gm lithofacies are interpreted analogously to the Modrová area as subaerial cohesive

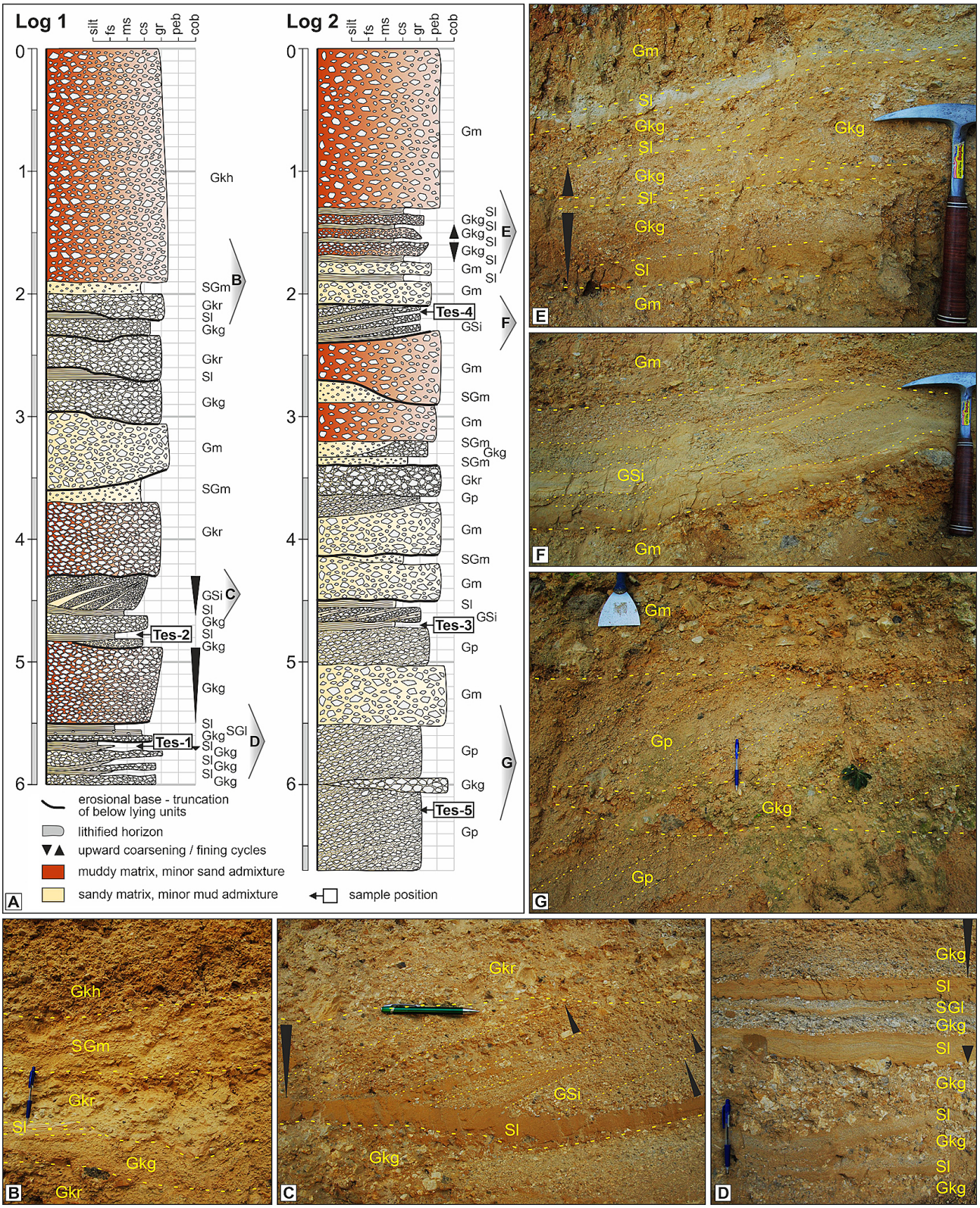

Fig. 12: Sedimentological log and photo documentation of the outcrop in abandoned quarry in the Tesáre locality with location of samples for granulometry and geochemistry. The nature of the outcrop allowed cleaning and recognition of eight lithofacies. Position of the logs is indicated on Fig. 11. For codes of lithofacies see Tab. 1 and for location see Fig. 2C.

debris flows with moderately high viscosity, or with low viscosity in the case of sand-dominated matrix (Nemec & Steel, 1984; Blikra & Nemec, 1998; Mulder & Alexander, 2001). The lithofacies SGm was most probably formed similarly by a low viscosity debris flow, considering its texture and sorting. The lithofacies Gkg is also analogously explained as a grain flow deposits with dominance of collisional stresses between grains as a motion factor (Lowe, 1976; Nemec & Steel, 1984; Nemec, 1990; Mulder & Alexander, 2001) and Gkr is considered as a rockfall deposit (Blikra & Nemec, 1998).

More than one third of the Tesáre outcrop succession (facies Gkh, Gp, GSi and Sl) is formed by traction current. The Gkh gravel with faint planar bedding is associated to unconfined sheetflow (Blikra & Nemec, 1998), which was potentially accumulated as upper-stage plane beds (Iseya & Ikeda, 1987; Cartigny et al., 2014).

The faintly planar cross-stratified moderately sorted gravel (Gp) is considered as a deposit of channelized traction current on a unit bar foreset (Bridge & Lunt, 2006; Reesink, 2018). Hence, its height between 15 and 64 cm should be equivalent to a channel depth, despite the uppermost part of a bar was probably eroded after its deposition. The facies exhibit slightly better sorting comparing to gravity flow deposits due to turbulence of traction current (e.g., Leclair, 2002; Baas et al., 2019). A similarity could be seen between the Gp facies and antidunes (e.g., Slootman & Cartigny, 2020). However, the palaeocurrent directions are generally oriented downslope from PI Mts. (Fig. 11C), implying progradation downstream. The lithofacies GSi is also considered as a bar deposits, but in a peripheral minor channel with increased variability in flow strength leading to cyclic deposition of gravelly normally graded strata and sandy mud lenses on the bar foreset (Miall, 2006). Nevertheless, this facies is not a common feature in an alluvial or colluvial fan environment and alternative explanation of its depositional process might exist.

Planar laminated muddy sand to sandy mud (Sl) was deposited by relatively slow traction current, implied by the high content of fine-grained fraction (Fig. 7). The deposit might be formed as drapes of migrating silty and sandy ripples in flow speed 0.3–0.5 $m \cdot s^{-1}$ under low sedimentation rate conditions (Yawar & Schieber, 2017).

Frequent presence of erosive surfaces is related to increased appearance of lithofacies deposited by traction currents. The turbulent flows with low concentration of sediment in comparison to debris flows or grain flows are prone to behave erosional. These flows were often in a bypass regime, forming only an erosional surface covered later by gravity flow deposits.

Several contradictory definitions of alluvial fan facies association were published, spanning from purely gravity flow dominated to purely alluvial environments (summarised in Plink-Björklund, 2021). This paper relies on the definition of colluvial fan as gravity flow dominated, alluvial fan as comprising both channelised traction current and gravity flow facies, and fluvial fan as an environment with dominance of channelized and overbank alluvial deposition. Hence, the depositional environment of the Tesáre outcrop is interpreted as an alluvial fan close to the transition towards a colluvial fan feeder of sediment (Blikra & Nemec, 1998). The gravity flow processes constitute approximately two thirds of the succession, while the rest is produced by redeposition of the debris flow, grain flow and rockfall deposits by a shallow braided river and sheetflow currents. As the term alluvial fan is used here to describe a facies association and not a morphological feature, evidence for a fan shape is not essential.

4.3 Petrography and geochemistry

The petrography of clasts of the Modrová Mb. is usually monotonous, depending on the composition of the nearby exposed pre-Cenozoic massifs. The Modrová area outcrops exhibit dolomitic composition (e.g., Modrová-1, 2 and Modrovka localities), or alteration of dolomitic and sandstone composition of gravel clasts (Lúka-1, 2 localities). The clast petrography indicates that provenance did not underwent significant change during the last ~8 Ma, since the same lithotypes could be find in close vicinity of the outcrops of colluvial fans. Mesoscopic observations of the Tesáre outcrop gravel material confirmed its dolomitic composition as well. A typical feature of the Modrová Mb. outcrops is the reddish colour of the muddy matrix.

4.3.1 Geochemistry of the gravel matrix from the Modrová-2 locality

Results of geochemistry applied to the fine-grained matrix (< 0.062 mm) of the Mod-3, Mod-4, Mod-5 and Mod-6 samples are included in the Tab. 2. The content of CaO (27–29 wt. %), MgO (19–20 wt. %), total carbon (11.8–12.6 wt. %) and CaO/MgO molar ratio (1.01–1.03) indicates presence of dolomite. This result is confirmed by the loss of volatile components (LOI 43–46%), which point to the presence of Ca-Mg carbonate (dolomite) instead to Ca-Mg oxide. After recalculation, dolomite form approximately 89–95 % of samples; the remaining oxides increase upwards from 4 wt. % (Mod-3) to 10 wt. % (Mod-6). They represent admixture of silicate minerals. Content of molar CaO, MgO and CO_2 implies that some carbonates contain also iron (ca. 0.7–1.7 %). Presence of organic carbon content is an alternative explanation, however, not favoured by the subaerial gravity flow origin of the studied sequence. Based on the described data, the groundmass of gravel is formed by detritic grains of dolomite with a small admixture of clay minerals (Fig. 13b).

The remarkable low content of terrigenous components prevents utilization of standard indexes used as palaeoclimatic and weathering proxies. Nevertheless, the calculated CIA index (Nesbitt & Young, 1982) after its simplification by McLennan (1993) provides values between 80–84; except for the sample Mod-3 (CIA = 42) (Fig. 13A; Tab. 2). The values indicate transition between moderate and intense degree of weathering. The sample Mod-3 is considered as an outlier due to extremely low CIA value, resulted likely from very low overall content of the analysed oxides. The enrichment factors (U, Fe, V, P) and Th/U ratio between 1–2 indicates redox conditions during deposition, but the assumption could be affected by the tendency of these elements to bound on carbonates. Therefore, they probably describe the depositional conditions of the primary carbonates and not the environment of colluvial fans. Other proxies could not be assessed due to the content of remaining oxides below the measurement limits.

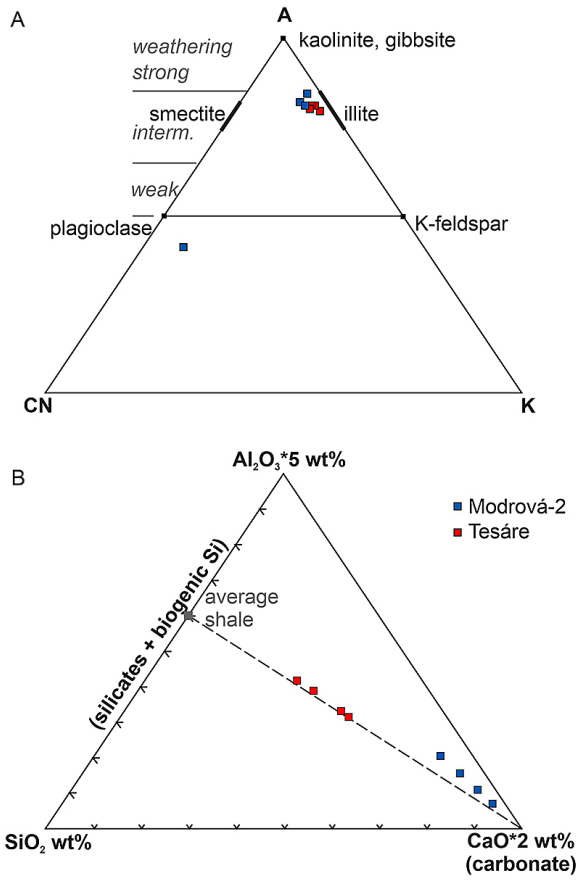

Fig. 13A: Plot of the CIA values for the matrix of samples from Modrová-2 and Tesáre localities in A-CN-K diagram (after Nesbitt & Young, 1984; Fedo et al. 1995). B: Diagram showing major components of matrix (after Brumsack 1989).

4.3.2 Geochemistry of the matrix of muddy sand samples from the Tesáre locality

Unlikely to the Modrová locality, analysis of the Tesáre samples showed lower content of carbonate documented by the LOI values ranging in 30–36% (Tab. 2). Presence of dolomite is indicated by content of CaO (16–21 wt. %), MgO (12–15 wt. %), total carbon (7–9 %) and values of CaO/MgO molar ratio in the range of 0.96–1.00. After recalculation, the lowest content of dolomite (53–59 wt. %) is established for the samples Tes-1 and Tes-2. The molar concentration of CaO and MgO of these samples corresponds to the molar concentration of CO_2. The remaining samples Tes-3 and Tes-4 contains approximately 68–70 wt. % of dolomite, but their molar concentration of CaO and MgO is lower comparing to the molar concentration of CO_2. This observation allows to assume that ~0.5 wt. % of the carbonates include Fe, or an unlikely option is presence of organic carbon in the sediment. Remaining oxides representing silicate minerals ranging from 27.5 to 36.6 wt. %, which allows for classification as clayey carbonate. Based on these results, the groundmass of studied gravel is formed by detritic grains of dolomite together with silicate minerals (Fig. 13B).

The SiO_2/Al_2O_3 ratio attaining values of 3.1–3.2 indicates clay admixture. The CIA index (Nesbitt & Young, 1982)

Tab. 2: Main bulk-rock geochemistry features of the samples from Modrová-2 and Tesáre localities. Enrichment factors were calculated as $(X_{sample}/Al_{sample})/(X_{UCC}/Al_{UCC})$. UCC after McLennan (2001). N.D. – sample under detection limite); * all Fe was measured as Fe_2O_3; + dolomite – CaO and MgO recalculated as $CaMg(CO_3)_2$; + rem. oxide – sum of oxides except CaO and MgO.

		Tes-1	Tes-2	Tes-5	Tes-6	Mod-3	Mod-4	Mod-5	Mod-6
SiO_2	%	23.73	26.84	19.22	18.09	1.65	2.57	3.74	5.14
TiO_2	%	0.32	0.36	0.24	0.26	0.03	0.07	0.10	0.15
Al_2O_3	%	7.55	8.51	5.98	5.55	0.87	1.48	2.17	3.06
*Fe_2O_3	%	3.32	3.77	2.6	2.33	0.29	0.59	0.73	1.03
Cr_2O_3	%	0.009	0.009	0.005	0.005	n.d.	n.d.	0.003	0.003
MgO	%	13.19	12.12	14.76	15.23	20.37	20.23	19.83	19.2
MnO	%	0.01	0.04	0.01	n.d.	n.d.	n.d.	n.d.	n.d.
CaO	%	17.91	16.38	20.56	21.24	29.31	28.85	28.03	27.16
Na_2O	%	0.07	0.09	0.08	0.09	0.31	0.03	0.04	0.03
K_2O	%	1.59	1.60	1.07	1.01	0.17	0.21	0.35	0.44
P_2O_5	%	0.09	0.26	0.30	0.21	0.70	0.02	0.02	0.03
LOI	%	31.9	29.7	34.9	35.7	46.0	45.6	44.6	43.4
Sum	%	99.72	99.72	99.69	99.69	99.65	99.63	99.65	99.65
Total C	%	7.73	6.96	8.87	9.11	12.63	12.40	12.03	11.79
Total/S	%	n.d.	n.d.	n.d.	n.d.	n.d.	n.d.	n.d.	n.d.
Co	ppm	3.5	4.4	2.9	2.4	0.7	0.9	1.2	1.9
Ga	ppm	7.8	8.3	4.8	5.2	n.d.	1.2	1.6	2.7
Hf	ppm	2.5	2.8	2.4	1.9	0.2	0.4	0.6	0.7
Rb	ppm	69.1	79.4	52.2	57.9	6.6	10.9	17.1	25.8
Sr	ppm	74.0	70.2	69.9	71.1	66.6	72.4	71.6	75.2
Ba	ppm	125.0	208.0	92.0	93.0	14.0	31.0	47.0	61.0
Th	ppm	5.6	7.1	4.2	3.9	0.7	0.9	1.3	2.1
U	ppm	2.7	2.6	1.7	1.7	0.6	0.5	0.7	0.9
V	ppm	69.0	74.0	53.0	53.0	9.0	20.0	24.0	36.0
Zr	ppm	90.6	111.9	88.0	69.0	8.3	14.8	20.6	28.1
CO_3	wt %	38.62	34.77	44.32	45.52	63.10	61.95	60.11	58.91
CO_2	mol %	0.64	0.58	0.74	0.76	1.05	1.03	1.00	0.98
CaO	mol %	0.32	0.29	0.37	0.38	0.52	0.51	0.50	0.48
MgO	mol %	0.33	0.30	0.37	0.38	0.51	0.51	0.50	0.48
CaO/MgO	mol ratio	0.97	0.96	0.99	1.00	1.03	1.02	1.01	1.01
dolomite	%	59.34	53.43	67.58	69.78	95.18	94.00	91.63	88.76
other carb.	%	0.00	0.00	0.51	0.15	1.77	1.19	0.72	1.75
CIA		79.36	80.64	80.64	79.80	40.89	81.71	80.75	84.06
SiO_2/Al_2O_3		3.14	3.15	3.21	3.26	1.90	1.74	1.72	1.68
Ga/Rb		0.11	0.10	0.09	0.09	0.00	0.11	0.09	0.10
K_2O/Al_2O_3		0.21	0.19	0.18	0.18	0.20	0.14	0.16	0.14
Th/U		2.07	2.73	2.47	2.29	1.17	1.80	1.86	2.33
U_{EF}		1.94	1.66	1.54	1.66	3.74	1.83	1.75	1.60
Co_{EF}		0.41	0.46	0.43	0.39	0.72	0.54	0.49	0.55
Fe_{EF}		1.33	1.34	1.32	1.27	1.01	1.21	1.02	1.02
V_{EF}		1.30	1.23	1.26	1.36	1.47	1.92	1.57	1.67
P_{EF}		1.13	2.89	4.75	3.58	76.20	1.28	0.87	0.93

after its simplification by McLennan (1993) varies in the range 79–80, implying that the feldspar weathering intensity reached the upper part of the moderate weathering zone. Production of illite during weathering is indicated by the K_2O/Al_2O_3 ratio of ~0.2 and Ga/Rb ratio of ~0.1, what supports either cold or dry climate. Illite production by weathering could be established also by visualization of values in the CIA plot (Fig. 13A; Tab. 2). Redox palaeoenvironmental conditions are implied by the enrichment factors (U, Fe, V, P) and by the U/Th ratio values of 2–3. As was mentioned earlier, this fact can be explained by binding of these elements to carbonate, since all Tesáre samples were deposited from traction current of a shallow stream.

4.3.3 Study of thin sections from the Lúka-2 locality

A lithified gravel sample taken from the Lúka-2 locality served for preparation of thin sections. Rounded gravel clasts of recrystallized, originally micritic carbonates and sparitic carbonates, occasionally with dispersed pyrite are the main detritic component (Fig. 14). Groundmass consists of detritic silt- to sand-sized grains composed mostly of quartz, carbonate grains, feldspar, chert, and mica (muscovite and biotite). Fragments of granitoids or gneiss are less frequent. The grains are cemented mainly by calcitic sparite; poikilitic calcite is less frequent, as shown by microprobe analysis (Fig. 15; Tab. 3, analyses 1, 2 and 4). Within sparite, dispersed crystals of dolomite are present (Tab. 3, analysis 6). Reddish colour of the groundmass implies the presence of iron oxides. Some of the clasts exhibit less distinct boundary to the cement and their colouring is more pronounced. It remains questionable if they comprise remnants of primary matrix or encompass a less stable clast type. The surface of some clasts is covered by clayey rim, which is formed probably by mixed-layer of montmorillonite/illite (Tab. 3, analyses 3 and 5).

5. STRUCTURAL POSITION OF THE MODROVÁ MB. ACCUMULATIONS

The geological mapping indicated that the occurrences of the Modrová Mb. are bound to marginal blocks of PI Mts. separated

Tab. 3: Results of electron probe analysis of cement present in the thin section. Carbonate analyses are recalculated to molecular wt. %.* - analyses of clay rims are recalculated based on 24 anions and normalised to 44 cation charge.

analyse	an1	an2	an4	an6		*an3	*an5
material	cement	cement	cement	dol. crystal		clay rims	
SiO_2	0.02	0.00	0.02	0.04	SiO_2	32.37	26.39
Al_2O_3	0.02	0.00	0.00	0.05	TiO_2	0.27	0.07
FeO	0.01	0.00	0.00	0.02	Al_2O_3	12.66	14.38
MgO	0.17	0.39	0.20	20.31	Cr_2O_3	0.00	0.01
MnO	0.04	0.02	0.00	0.02	FeO	2.96	3.18
CaO	54.50	54.58	55.36	32.27	MgO	3.10	1.81
SrO	0.01	0.00	0.04	0.01	MnO	0.00	0.00
SO_2	0.03	0.03	0.03	0.01	NiO	0.00	0.00
Total	54.78	55.03	55.65	52.73	CaO	4.80	6.43
$FeCO_3$	0.01	0.01	0.00	0.03	K_2O	3.98	2.70
$MgCO_3$	0.35	0.82	0.42	42.49	Na_2O	0.07	0.11
$MnCO_3$	0.06	0.03	0.00	0.03	Cl	0.30	0.58
$CaCO_3$	97.27	97.42	98.80	57.60	F	0.00	0.00
$SrCO_3$	0.01	0.00	0.05	0.02	Total	60.51	55.66
SiO_2	0.02	0.00	0.02	0.04	Si	6.956	6.283
Al_2O_3	0.04	0.00	0.00	0.10	^TAl	1.044	1.717
S	0.01	0.02	0.01	0.00	Sum	8.000	8.000
Sum	97.77	98.30	99.32	100.31	Al	2.163	2.319
					Ti	0.043	0.013
					Fe^{2+}	0.532	0.633
					Mg	0.993	0.641
					Mn	0.000	0.000
					Cr	0.000	0.003
					Ni	0.000	0.000
					sum	3.732	3.610
					Ca	1.105	1.641
					K	1.092	0.819
					Na	0.029	0.049
					sum	2.226	2.509

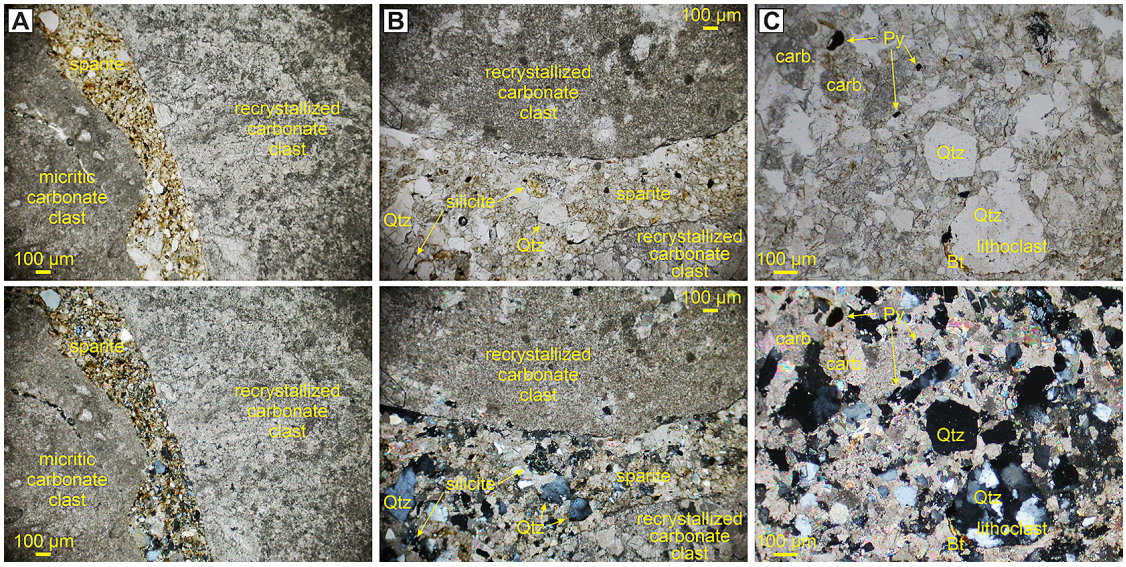

Fig. 14: Thin section images from the Lúka-2 locality showing detritic grains and matrix. Upper photos represent plane polarised light, lower photos cross polarised light. Abbreviations: Qtz – quartz; Bt – biotite; carb. – detritic carbonate.

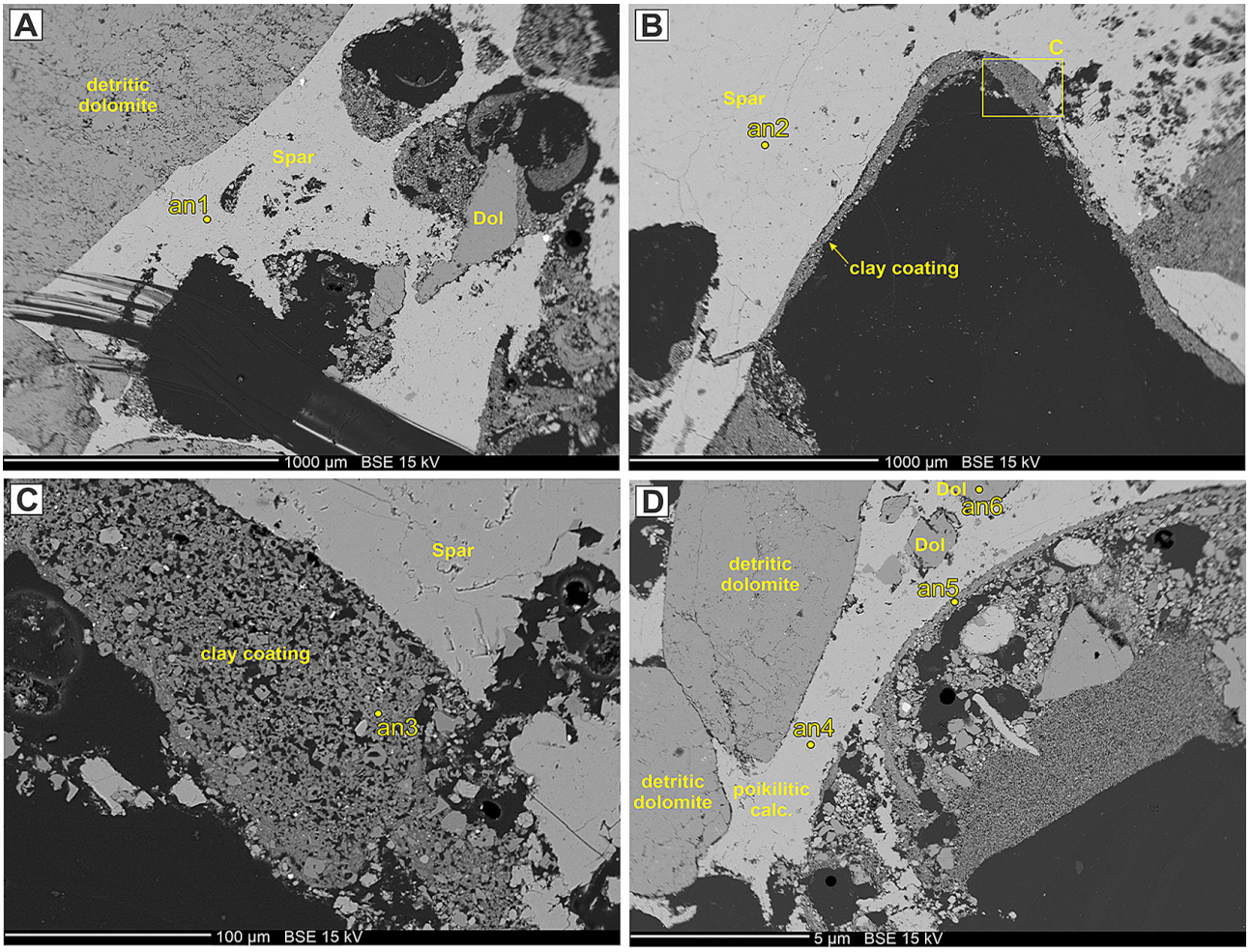

Fig. 15: Positions of the electron probe analyses within a thin section from the Lúka-2 locality. Dol - dolomite; Spar - calcitic sparite.

from the central one by faults (Ivanička et al., 2007). Despite the exact fault-slip data are not available, the geophysical data shows that PI Mts. horst is markedly bounded by normal faults (Bielik et al., 2002; Bezák et al., 2014; Marko et al., 2017; Pašteka et al., 2017). Large-scale Cenozoic normal faults are evident also in the internal structure of the horst, e.g. displacing structurally lowermost Tatric crystalline basement to the proximity of the structurally higher Fatric and Hronic sequences (Fig. 2A).

Geological and geophysical evidence of blocks with an uplift history different from the main (central) block of the mountain range are relatively well seen in the area between the Hrádok and Hubina villages on the western flank of PI Mts. (Modrová area). Especially the Bouger anomaly horizontal gravity gradient and "tilt" derivation transformed map (Fig. 7 in Marko et al., 2017) show strong N–S linear anomalies following fault contact of the Mesozoic and/or Paleogene formations with the Miocene sediments (Fig. 16). Strong NE–SW anomalies in the derived Bouguer gravity map as well as the distribution of the Modrová, Ducové and Hlavina members located between the Ducové and Modrová villages (Fig. 2B) suggest that this block experienced different uplift history than the main block of the mountain range during the late Miocene.

Similar situation is seen in the area of Tesáre village, however, not such clear as in the area of Modrová. It is caused by the more complicated Miocene tectonic history, that involves the existence of repeatedly uplifted and buried Závada-Bielice Rise (Fig. 1 and 16) (Vass et al., 2002) which is roughly perpendicular to the Považský Inovec Mts. horst. The interpretation of the geophysical signal (Fig. 16) (Marko et al., 2017) is not straightforward. Nevertheless, it can be stated that the younger NNE–SSW (to E–W) normal fault interferes with the older faults of NNW–SSE trend.

The geological section on the Fig. 17 located on the western margin of the mountains depicts the general structure of the Modrová area in relation to the central block of PI Mts. and to the Blatné depression. The block, which comprise the northern part of the Blatné depression contains the succession of lower Miocene deposits covered by the Quaternary alluvial gravel. It could be assumed that the upper Miocene deposits were eroded from this area by the Váh River during Quaternary.

6. PALAEOENVIRONMENTAL AND PALAEOGEOGRAPHIC INTERPRETATION

The accumulation of the colluvial and alluvial fans of the Modrová Mb. clearly indicate the presence of exposed slopes consisting of Mesozoic dolomites and Paleogene siliciclastics.

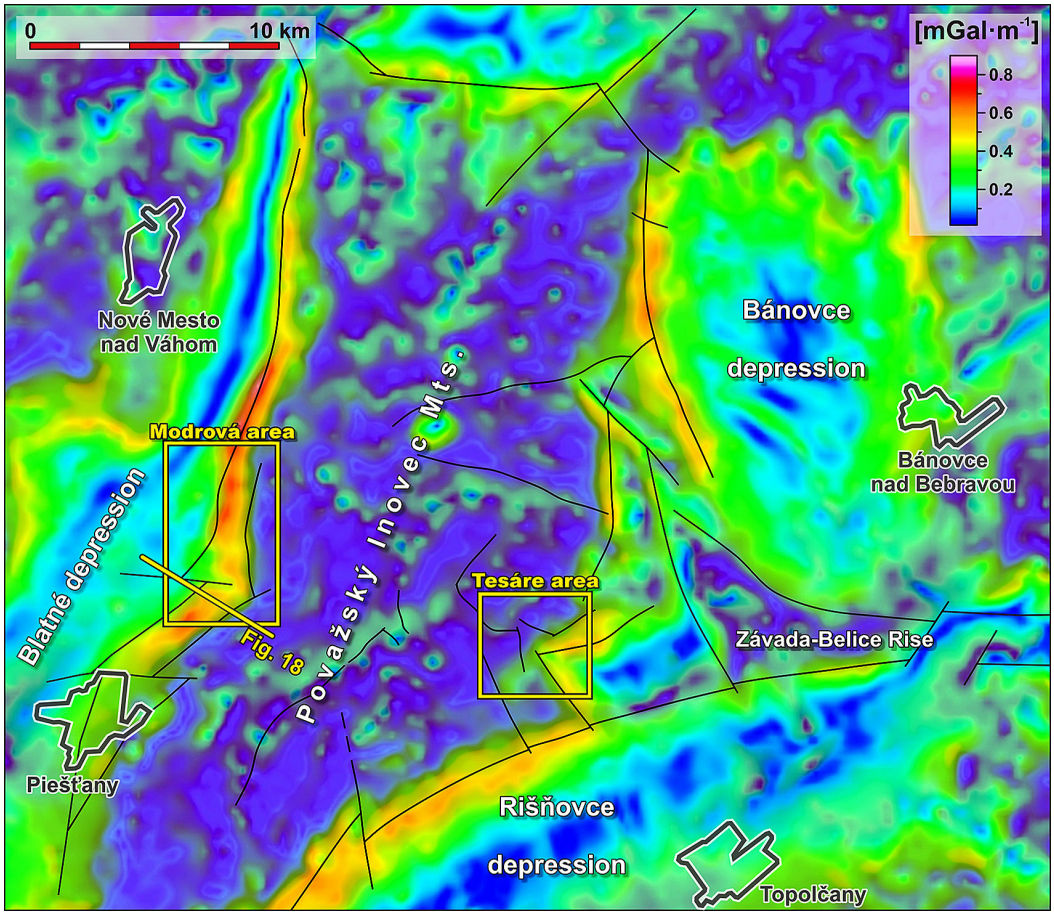

Fig. 16: Bouger anomaly horizontal gravity gradient and "tilt" derivation transformed map (modified from Marko et al., 2017) with indication of interpreted faults, which serve as an evidence for the blocky structure of the Modrová and Tesáre areas separated from the main block of the Považský Inovec Mts. Grey polygons represent towns.

The blocky structure of the marginal parts of PI Mts. (where Modrová Mb. appears) provide an explanation of these slopes as scarps of marginal faults. Differential movements must have been appeared around 8 Ma. These fault movements were in the order of tens of meters and most likely did not exceed ~ 100 m. The tentative estimation of fault-slip is supported by the overall low thickness of the Modrová Mb. (first tens of meters) and by the absence of dolomite and sandstone clasts (material of the Modrová Mb.) in contemporaneous deposits of the Piešťany Mb. in the Blatné depression, as well as in the alluvial fill of the Rišňovce depression (Šujan et al., 2017). Higher scarps between the central and marginal blocks would cause supply of coarse-grained clastics, which would be recognised in the depositional record of surrounding basins.

The Modrová area comprised mostly colluvial fans, which were supplied enough just to fill the accommodation above the marginal tectonic block (Fig. 18). The transition to alluvial fan depositional processes was probably located on the margin to the Blatné depression, where alluvial redistribution by the palaeo-Váh river dominated. The colluvial fans coexisted with deposition of the terrestrial carbonates of the Hlavina Mb. and its feeder system was bounded to the active faults. Active tectonics commonly causes synchronous deposition of colluvial and freshwater limestone (travertine) facies, as was shown for example in Croci et al. (2016) and Wang et al. (2016).

The depositional record of alluvial fan facies was documented in the Tesáre area, close to the transition to the Rišňovce depression. The occurrence of more distal facies association in comparison to the Modrová area leads to assumption, that the accommodation was more spatially extensive to allow preservation of more distal facies on this marginal block of PI Mts. It might be caused by more gentle slopes, higher distance to the marginal faults, or simply by a position of the studied succession in a watershed of a permanent stream (Blikra & Nemec, 1998). Transition towards more distal depositional environment of a stream with larger provenance area is illustrated by the shift of position between Modrová-2 and Tesáre samples on the plot of major matrix components on Fig. 13B.

Mean annual precipitation (MAP) decreased in the region

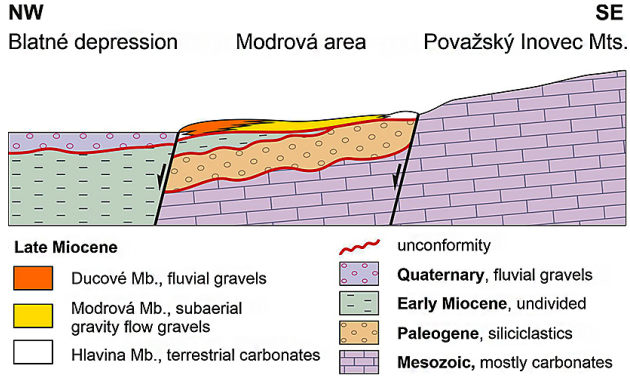

Fig. 17: Generalised geological section across the Modrová area. For location see Fig. 2 and 16.

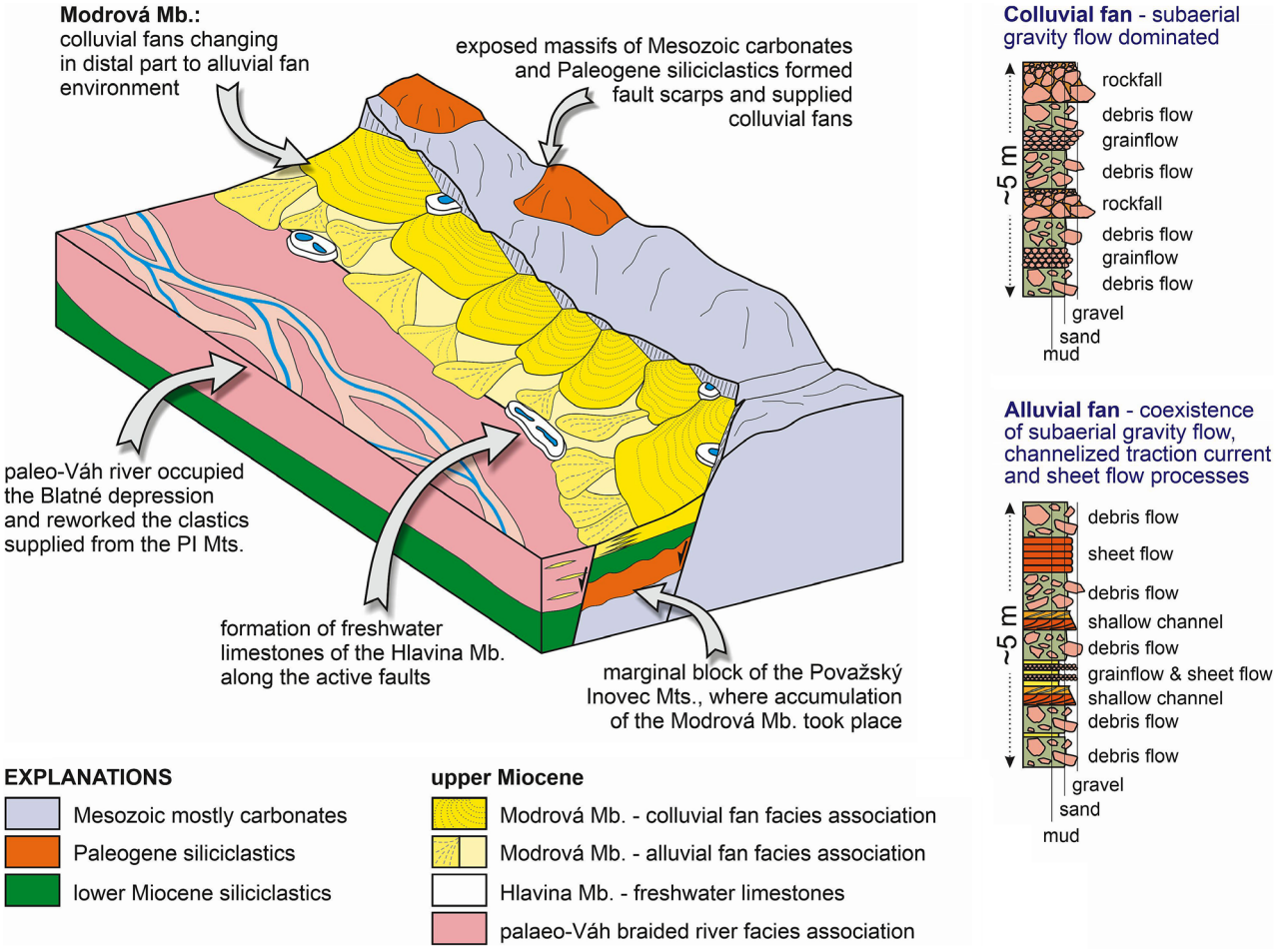

Fig. 18: Palaeogeographic scheme of the Modrová area at ~8 Ma with depositional environment of the Modrová Mb. and sedimentological logs showing characteristic lithofacies and depositional processes. For location see Fig. 2 or Fig. 16.

from "washhouse" climate around 10 Ma with values of 1000–1500 mm (Böhme et al., 2008; 2011; Kováčová et al., 2011) to 500–1000 mm (Böhme et al., 2011) or ~800 mm (van Dam, 2006) around 8 Ma. It was suggested that the decrease in precipitation might be related to the regression of Lake Pannon (Utescher et al., 2017), since distance to its water masses would strongly affect precipitation intensity. Mean annual temperature (MAT) at ~8 Ma reached 15–17 °C (Prista et al., 2015). Hence, the regional palaeoclimate during the deposition of the Modrová Mb. was of similar humidity and with higher MAT in comparison to the recent conditions reaching MAP of 500–600 mm and MAT of 9–11°C (Mello et al., 2007; 2013).

Geochemical proxies of the Modrová Mb. implied either cold or dry conditions, what contradicts to the published estimates for the region and time period. However, the geochemical proxies were analysed in this study on a minor siliciclastic fraction of the sediments dominated by carbonates (Fig. 13B). Moreover, the colluvial to alluvial fan facies were accumulated rapidly from the exposed and weathered rock massifs. Hence, it could be assumed that the degree of weathering to illite is caused mostly by rapid denudation conditions, what biased the informative value of palaeoclimatic proxies in the studied samples.

The dominance of the debris flow facies within gravity flow deposits and common presence of sheet flow processes also indicate humid conditions (Blikra & Nemec, 1998; Nemec & Kazanci, 1999). The reddish colour of the matrix is associated with presence of iron oxides and clay coatings around the clastic grains, what might be related to fersiallitic weathering typical for warm and humid climate with dry seasons (Duchaufour, 1977). The oxidation of pyrite, which is scattered within the matrix of clastic carbonates, contributed to formation of the reddish colouring of the matrix and rims of the detritic grains.

A comparable facies association of alluvial fan to braided river conglomerates with reddish matrix was documented as the upper Miocene Rohrbach Fm. in the southwestern tip of the Vienna Basin, eastern Austria (Koukal & Wagreich, 2009). The Diás Fm. is another succession with similar facies of subaerial gravity flow and braided river origin, present in the Keszthely Mts. north of Lake Balaton in the western Hungary (Budai et al., 1999). It accumulated mostly as alluvial fans preceding the transgression of Lake Pannon, which appeared in the area at ca. 8.8–8.5 Ma (Sztanó et al., 2013). The sediment supply from slopes was predisposed by scarps of active faults (Csillag et al., 2010). Colluvial deposits with comparable lithology and of the supposed late Miocene age were identified in the Turiec Basin in the Central Western Carpathians (Kováč et al., 2011b). The simultaneous appearance of such successions across the Western Carpathian

realm might point to a mild regional phase of tectonic activity, which could be explored in detail by future studies focused on the margins of the mountains towards the surrounding basins elsewhere in the region.

On the basis of regional conditions and characteristics of the studied deposits, described facies associations of colluvial and alluvial fans point to active tectonics in a warm and humid climate. The study aims to emphasize the potential of colluvial and alluvial fan sediments as indicators of palaeoenvironmental and palaeogeographic conditions in terrestrial environments.

7. CONCLUSIONS

The marginal blocks of the Považský Inovec Mts. (PI Mts.), which are separated from the main mountain horst by faults, accommodated coarse clastics of the Modrová Mb. The strata were deposited around 8 Ma according to their lateral transitions with freshwater limestones of the Hlavina Mb., dated in previous studies by rodent biostratigraphy (e.g., Kováč et al., 2011a). Facies analysis revealed a colluvial fan origin of the studied deposits in the western margin of PI Mts., with prevalence of cohesive debris flow facies and occurrence of rockfall, grain flow and sheet flow processes. The Tesáre area located on the eastern margin of the mountains comprise alluvial fan deposits accumulated by debris flows, by traction currents in a shallow braided river and sheet flow processes.

Fault activity on the margins of the tectonic blocks caused sediment supply capable of filling the accommodation on the blocks. However, its relatively low intensity led to the dominance of alluvial redeposition of the sediment delivered to the surrounding Blatné and Rišňovce depressions of the Danube Basin, as was observed in Šujan et al. (2017). Hence, a tentative estimate for fault-slip between the marginal blocks and the main horst of PI Mts. is in the range of tens of meters.

The deposit is dominated by dolomite clastics, as documented by thin section study, geochemistry and probe analysis. Geochemical proxies applied to the matrix of clastic sediment implied either cold or dry climate, what contradicts to the data published for the region and time period (e.g., Böhme et al., 2011; Prista et al., 2015). The weathering to illite is explained as a result of rapid denudation, which limits the application of these proxies. Facies associations imply a humid climate with surficial runoff caused by heavy rains. The presence of clay coatings of sediment grains and iron oxides in the matrix is interpreted as a result of fersiallitic weathering and oxidation of pyrite dispersed in the matrix, what fits well to a humid and warm climate.

Several comparable successions were described in the region, e.g., in the southwestern Vienna Basin (Rohrbach Fm., Koukal & Wagreich, 2009), in the Transdanubian Range (Diás Fm., Budai et al., 1999; Csillag et al., 2010) and also in the Turiec Basin (Kováč et al., 2011b). It remains questionable, if comparable accumulations are present also on transitions of other morphostructural elevations towards neighboring basins of the Western Carpathians, what might point to a mild but regional phase of fault activity.

Acknowledgements: This work was financially supported by the Slovak Research and Development Agency under contracts No's APVV-0099-11, APVV-14-0118, APVV-15-0575, APVV-16-0121 and SK-HU-2013-0020. The Hungarian colleagues are thanked for the co-operation on the bilateral project SK-HU-2013-0020, which allowed us to observe facies comparable to the subject of this study during a field trip around Lake Balaton. Especially, Gábor Csillag and Orsolya Sztanó provided very helpful insight into the character of the Diás Fm. Thanks goes to Rastislav Vojtko for providing shapefiles of the general geological map. The manuscript benefited highly from the comments and suggestions done by the reviewers Andrei Matoshko and Ľubomír Sliva, as well as from helpful editing done by Rastislav Vojtko.

References

Baas, J.H., Baker, M.L., Malarkey, J., Bass, S.J., Manning, A.J., Hope, J.A., Peakall, J., Lichtman, I.D., Ye, L., Davies, A.G., Parsons, D.R., Paterson, D.M. & Thorne, P.D., 2019: Integrating field and laboratory approaches for ripple development in mixed sand–clay–EPS. *Sedimentology* 66, 2749–2768.

Bagnold, R.A., 1954: Experiments on a gravity-free dispersion of large solid spheres in a Newtonian fluid under shear. *Proceedings of the Royal Society of London* A255, 49–63.

Balázs, A., Matenco, L., Magyar, I., Horváth, F. & Cloetingh, S., 2016: The link between tectonics and sedimentation in back-arc basins: New genetic constraints from the analysis of the Pannonian Basin. *Tectonics* 35, 1526–1559.

Beidinger, A. & Decker, K., 2011: 3D geometry and kinematics of the Lassee flower structure: Implications for segmentation and seismotectonics of the Vienna Basin strike–slip fault, Austria. *Tectonophysics* 499, 22–40.

Bezák, V., Pek, J., Vozár, J., Bielik, M. & Vozár, J., 2014: Geoelectrical and geological structure of the crust in Western Slovakia. *Studia Geophysica et Geodaetica* 58, 473–488.

Bielik, M., Kováč, M., Kučera, I., Michalík, P., Šujan, M. & Hók, J., 2002: Neoalpine linear density boundaries (faults) detected by gravimentry. *Geologica Carpathica* 53, 235–244.

Blair, T.C. & McPherson, J.G., 1994: Alluvial fans and their natural distinction from rivers based on morphology, hydraulic processes, sedimentary processes, and facies assemblages. *Journal of Sedimentary Research* 64, 450–489.

Blikra, L.H. & Nemec, W., 1998: Postglacial colluvium in western Norway: depositional processes, facies and palaeoclimatic record. *Sedimentology* 45, 909–959.

Böhme, M., Ilg, A. & Winklhofer, M., 2008: Late Miocene "washhouse" climate in Europe. *Earth and Planetary Science Letters* 275, 393–401.

Böhme, M., Winklhofer, M. & Ilg, A. 2011: Miocene precipitation in Europe: Temporal trends and spatial gradients. *Palaeogeography, Palaeoclimatology, Palaeoecology* 304, 212–218.

Bridge, J.S. & Lunt, I.A., 2006: Depositional models of braided rivers, in: Sambrook Smith, G.H., Best, J.L., Bristow, C.S. & Petts, G.E. (Eds.): Braided Rivers: Process, Deposits, Ecology and M anagement. International Association of Sedimentologists Special Publication, Wiley-Blackwell, Oxford, pp. 396.

Brixová, B., Mosná, A. & Mojzeš, A., 2018a: Geophysical research of the Western Carpathians faults - Sološnica (case study). *EGRSE* 25, 2, 12–19.

Brixová, B., Mosná, A. & Putiška, R., 2018b: Applications of Shallow Seismic Refraction Measurements in the Western Carpathians (Slovakia): Case Studies. *Contributions to Geophysics and Geodesy* 48, 1, 1–21.

Brumsack, H.J., 1989: Geochemistry of recent TOC-rich sediments from the Gulf of California and the Black Sea. *Geologische Rundschau* 78, 851–882.

Budai, T., Császár, G., Csillag, G., Dudko, A., Koloszár, L. & Majoros, Gy., 1999: Geology of the Balaton Highland. Explanation to the Geological Map of the Balaton Highland, 1: 50 000. Geological Institute of Hungary, Budapest, pp. 210.

Cartigny, M.J.B., Ventra, D., Postma, G. & van Den Berg, J.H., 2014: Morphodynamics and sedimentary structures of bedforms under supercritical-flow conditions: New insights from flume experiments. *Sedimentology* 61, 712–748.

Costa, J.E., 1988: Rheologic, geomorphic, and sedimentologic differentiation of water floods, hyperconcentrated flows, and debris flows. In: Baker, V.R., Kochel, R.C., Patton, P.C., (Eds.): Flood geomorphology. John Wiley and Sons, New York, pp. 113–122.

Croci, A., Della Porta, G. & Capezzuoli, E., 2016: Depositional architecture of a mixed travertine-terrigenous system in a fault-controlled continental extensional basin (Messinian, Southern Tuscany, Central Italy). *Sedimentary Geology* 332, 13–39.

Csillag, G., Sztanó, O., Magyar, I. & Hámori, Z., 2010: Stratigraphy of the Kálla Gravel in Tapolca Basin based on multi-electrode probing and well data. *Földtani Közlöny* 140, 183–196 (in Hungarian with English abstract).

Danišík, M., Dunkl, I., Putiš, M., Frisch, W. & Kráľ, J., 2004: Tertiary burial and exhumation history of basement highs along the NW margin of the Pannonian Basin – an apatite fission track study. *Australian Journal of Earth Sciences* 95–96, 60–70.

de Haas, T., Ventra, D., Carbonneau, P.E. & Kleinhans, M.G., 2014: Debris-flow dominance of alluvial fans masked by runoff reworking and weathering. *Geomorphology* 217, 165–181.

Duchaufour, P., 1977: Pedology: Pedogenesis and Classification. Allen & Unwin, London, 448 pp.

Fedo, Ch.M., Nesbitt, H.W. & Young, G.M., 1995: Unraveling the effects of potassium metasomatism in sedimentary rocks and paleosols, with implications for paleoweathering conditions and provenance. *Geology* 23, 921–924.

Folk, R.L. & Ward, W.C., 1957: A Study in the Significance of Grain-Size Parameters. *Journal of Sedimentary Petrology* 27, 3–26.

Fordinál, K. & Elečko, M., 2000: Ripňany Formation – a Sarmatian and Early Pannonian fresh water sedimentary assemblage of the Rišňovce depression. *Mineralia Slovaca* 32, 46–55.

Havrila, M., 2011: Hronikum: paleogeografia a stratigrafia (vrchný pelsón – tuval), štrukturalizácia a stavba. *Geologické práce, Správy* 117, 7–103.

Hók, J., Šujan, M. & Šipka, F., 2014: Tectonic division of the Western Carpathians: An overview and a new approach. *Acta Geologica Slovaca* 6, 135–143.

Horváth, F., Bada, G., Szafián, P., Tari, G., Ádám, A. & Cloetingh, S., 2006: Formation and deformation of the Pannonian Basin: Constraints from observational data. In: Gee, D.G. & Stephenson, R.A. (Eds.): European Lithosphere Dynamics. Geological Society, London, Memoirs 32, pp. 191–206.

Iseya, F. & Ikeda, H., 1987: Pulsations in bedload transport rates induced by a longitudinal sediment sorting: a flume study using sand and gravel mixtures. *Geografiska Annaler* 69, 15–27.

Ivanička, J., Havrila, M., Kohút, M., Kováčik, M., Madarás, J., Olšavský, M., Hók, J., Polák, M., Filo, I., Elečko, M., Fordinál, K., Maglay, J., Pristaš, J., Buček, S. & Šimon, L., 2007: Geologická mapa Považského Inovca a jv. časti Trenčianskej kotliny 1: 50 000. Štátny geologický ústav Dionýza Štúra a Ministerstvo životného prostredia, Bratislava.

Ivanička, J., Kohút, M., Havrila, M., Olšavský, M., Hók, J., Kováčik, M., Madarás, J., Polák, M., Rakús, M., Filo, I., Elečko, M., Fordinál, K., Maglay, J., Pristaš, J., Buček, S., Šimon, L., Kubeš, P., Scherer, S., Zuberec, J., Dananaj, I. & Klukanová, A., 2011: Vysvetlivky ku geologickej mape Považského Inovca a J.V. časti Trenčianskej kotliny 1: 50 000. Štátny geologický ústav Dionýza Štúra, Bratislava.

Iverson, R.M., 1997: The physics of debris flows. *Reviews of Geophysics* 35, 245–296.

Klučiar, T., Kováč, M., Vojtko, R., Rybár, S., Šujan, M. & Králiková, S., 2016: The Hurbanovo–Diösjenő Fault: A crustal-scale weakness shear zone at the boundary of the Central estern Carpathians and Northern Pannonian Domain. *Acta Geologica Slovaca* 8, 59–70.

Koukal, V. & Wagreich, M., 2009: Sedimentology and Definition of the Rohrbach Formation ("Rohrbacher Conglomerate", Upper Miocene – Pliocene) in the Quarry of Rohrbach/Ternitz (Lower Austria). *Jahrbuch der Geologischen Bundesanstalt* 149, 453–462.

Kováč, M., 2000: Geodynamický, paleogeografický a štruktúrny vývoj Karpatsko-Panónskeho regiónu v miocéne: nový pohľad na neogénne panvy Slovenska. Veda, Slovac Academy of Sciences, Bratislava, 204 pp.

Kováč, M., Halásová, E., Hudáčková, N., Holcová, K., Hyžný, M., Jamrich, M. & Ruman, A., 2018b: Towards better correlation of the Central Paratethys regional time scale with the standard geological time scale of the Miocene Epoch. *Geologica Carpathica* 69, 283–300.

Kováč, M., Král, J., Márton, E., Plašienka, D. & Uher, P., 1994: Alpine uplift history of the central western Carpathians: geochronological, paleomagnetic, sedimentary and structural data. *Geologica Carpathica* 45, 83–96.

Kováč, M., Márton, E., Klučiar, T. & Vojtko, R., 2018a: Miocene basin opening in relation to the north-eastward tectonic extrusion of the ALCAPA Mega-Unit. *Geologica Carpathica* 69, 254–263.

Kováč, M., Márton, E., Oszczypko, N., Vojtko, R., Hók, J., Králiková, S., Plašienka, D., Klučiar, T., Hudáčková, N. & Oszczypko-Clowes, M., 2017: Neogene palaeogeography and basin evolution of the Western Carpathians, Northern Pannonian domain and adjoining areas. *Global and Planetary Change* 155, 133–154.

Kováč, M., Hók, J., Minár, J., Vojtko, R., Bielik, M., Pipík, R., Rakús, M., Kráľ, J., Šujan, M., Králiková, S., 2011b: Neogene and Quaternary development of the Turiec Basin and landscape in its catchment: A tentative mass balance model. *Geologica Carpathica* 62, 361–379.

Kováč, M., Synak, R., Fordinál, K., Joniak, P., Tóth, C., Vojtko, R., Nagy, A., Baráth, I., Maglay, J. & Minár, J., 2011a: Late Miocene and Pliocene history of the Danube Basin: Inferred from development of depositional systems and timing of sedimentary facies changes. *Geologica Carpathica* 62, 519–534.

Kováčová, M., Doláková, N. & Kováč, M., 2011: Miocene vegetation pattern and climate change in the northwestern Central Paratethys domain (Czech and Slovak Republic). *Geologica Carpathica* 62, 251–256.

Králiková, S., Vojtko, R., Hók, J., Fügenschuh, B. & Kováč, M., 2016: Low-temperature constraints on the Alpine thermal evolution of the Western Carpathian basement rock complexes. *Journal of Structural Geology* 91, 144–160.

Kušnirák, D., Hermann, Z., Bielik, M., Putiška, R., Mojzeš, A., Brixová, B., Pašteka, R., Dostál, I., Zahorec, P., Papčo, J., Hók, J., Bošanský, M. & Krajnak, M., 2020: Physical properties of Hradiste border fault (Turiec Basin, Western Carpathians, Slovakia) inferred by multidisciplinary geophysical approach. *Geologica Carpathica* 71, 1, 3–13.

Lačný, A., Bella, P., Velšmid, M. & Csibri, T., 2020: The Večerná-Čárka cave system (Kuchyňa-Orešany Karst, Malé Karpaty Mountains, Slovakia) – tectonically controlled phreatic speleogenesis in the marginal part of block mountains. *Acta Geologica Slovaca* 12, 1–13.

Lačný, A., Kubičina, L. & Csibri, T., 2019: Morphometric analysis of sinkholes on the Čachtická Plain. *Acta Carsologica Slovaca* 57, 147–164.

Leclair, S.F., 2002: Preservation of cross-strata due to the migration of subaqueous dunes: An experimental investigation. *Sedimentology* 49, 1157–1180.

Legros, F., 2002: Can dispersive pressure cause inverse grading in grain flows? *Journal of Sedimentary Research* 72, 166–170.

Lenhardt, W.A., Švancara, J., Melichar, P., Pazdírková, J., Havíř, J. & Sýkorová, Z., 2007: Seismic activity of the Alpine-Carpathian-Bohemian Massif region with regard to geological and potential field data. *Geologica Carpathica* 58, 397–412.

Longhitano, S.G., Sabato, L., Tropeano, M., Murru, M., Carannante, G., Simone, L., Cilona, A. & Vigorito, M., 2015: Outcrop reservoir analogous and porosity changes in continental deposits from an extensional basin: The case study of the upper Oligocene Sardinia Graben System, Italy. *Marine and Petroleum Geology* 67, 439–459.

Lowe, D.R., 1976: Grain flow and grain flow deposits. *Journal of Sedimentary Research* 46, 188–199.

Marko, F., Andriessen, P.A.M., Tomek, Č., Bezák, V., Fojtíková, L., Bošanský, M., Piovarči, M. & Reichwalder, P., 2017: Carpathian Shear Corridor – A strike-slip boundary of an extruded crustal segment. *Tectonophysics* 703–704, 119–134.

McLennan, S.M., 1993: Weathering and global denudation. Journal of Geology 101, 295–303.

McLennan, S.M., 2001: Relationships between the trace element composition of sedimentary rocks and upper continental crust. *Geochemistry, Geophysics, Geosystems* 2, 2000GC000109.

Melo, M., Lapin, M. & Damoborská, I., 2007: Detection of climatic trends and variability at Hurbanovo. In: Střelcová, K., Škvarenina, J. & Blaženec, M., (Eds.): Bioclimatology and Natural Hazards, International Scientific Conference, Poľana nad Detvou, Slovakia.

Melo, M., Lapin, M., Kapolková, H., Pecho, J. & Kružicová, A., 2013: Climate Trends in the Slovak Part of the Carpathians. In: Kozák, J. (Ed.): The Carpathians: Integrating Nature and Society Towards Sustainability, Environmental Science and Engineering. Springer-Verlag, Berlin, pp. 131–150.

Merritts, D.J., Vincent, K.R. & Wohl, E.E., 1994: Long river profiles, tectonism, and eustasy: a guide to interpreting fluvial terraces. *Journal of Geophysical Research* 99, 14031–14050.

Miall, A.D., 2006: The geology of fluvial deposits: Sedimentary facies, basin analysis, and petroleum geology, 3rd edition ed. Springier, Berlin.

Minár, J., Bielik, M., Kováč, M., Plašienka, D., Barka, I., Stankoviansky, M. & Zeyen, H., 2011: New morphostructural subdivision of the Western Carpathians: An approach integrating geodynamics into targeted morphometric analysis. *Tectonophysics* 502, 158–174.

Mulder, T. & Alexander, J., 2001: The physical character of subaqueous sedimentary density flow and their deposits. *Sedimentology* 48, 269–299.

Nelson, A.R., 1992: Lithofacies analysis of colluvial sediments - an aid in interpreting the recent history of Quaternary normal faults in the Basin and Range Province, western United States. *Journal of Sedimentary Petrology* 62, 607–621.

Nemec, W., 1990: Aspects of sediment movement on steep delta slopes, in: Colella, A. & Prior, D.B. (Eds.): Coarse-Grained Deltas. *IAS Special Publication* 10, pp. 29–73.

Nemec, W. & Kazanci, N., 1999: Quaternary colluvium in west-central Anatolia: Sedimentary facies and palaeoclimatic significance. *Sedimentology* 46, 139–170.

Nemec, W. & Steel, R.J., 1984: Alluvial and coastal conglomerates: their significant features and some comments on gravelly mass flow deposits, in: Koster, E.H. & Steel, R.J. (Eds.): Sedimentology of Gravels and Conglomerates. *Memories of the Canadian Society of Petroleum Geologists*, pp. 1–30.

Nesbitt, H.W. & Young, G.M., 1982: Early proterozoic climates and plate motions inferred from major element chemistry of lutites. *Nature* 299, 715–717.

Nesbitt, H.W. & Young, G.M., 1984: Prediction of some weathering trends of plutonic and volcanic rocks based on thermodynamic and kinetic considerations. *Geochimica et Cosmochimica Acta* 48, 1523–1534.

Pašteka, R., Zahorec, P., Kušnirák, D., Bošanský, M., Papčo, J., Szalaiová, V., Krajňák, M., Ivan, M., Mikuška, J. & Bielik, M., 2017: High resolution Slovak Bouguer gravity anomaly map and its enhanced derivative transformations: New possibilities for interpretation of anomalous gravity fields. *Contributions to Geophysics and Geodesy* 47, 81–94.

Plašienka, D., Méres, Š., Ivan, P., Sýkora, M., Soták, J., Lačný, A., Aubrecht, R., Bellová, S. & Potočný, T., 2020: Meliatic blueschists and their detritus in Cretaceous sediments: new data constraining tectonic evolution of the West Carpathians. *Swiss Journal of Geosciences* 112, 55–81.

Plink-Björklund, P., 2021: Distributive Fluvial Systems: Fluvial and Alluvial Fans. In: Alderton, D. & Elias, S.A. (Eds.): Encyclopedia of Geology (Second Edition). Academic Press, Oxford, pp. 745–758.

Prista, G.A., Agostinho, R.J. & Cachão, M.A., 2015: Observing the past to better understand the future: A synthesis of the Neogene climate in Europe and its perspectives on present climate change. *Open Geosciences* 7, 65–83.

Prokešová, R., Plašienka, D. & Milovský, R., 2012: Structural pattern and emplacement mechanisms of the Krížna cover nappe (Central Western Carpathians). *Geologica Carpathica* 63, 13–32.

Putiška, R., Kušnirák, D., Dostál, I., Lačný, A., Mojzeš, A., Hók, J., Pašteka, R., Krajňák, M. & Bošanský, M., 2014: Integrated geophysical and geological investigations of karst structures in komberek, Slovakia. *Journal of Cave and Karst Studies* 76, 155–163.

Reesink, A.J.H., 2018: Interpretation of cross strata formed by unit bars, in: Ghinassi, M., Colombera, L., Mountney, N.P. & Reesink, A.J.H. (Eds.): Fluvial Meanders and Their Sedimentary Products in the Rock Record. International Association of Sedimentologists Special Publication, Wiley-Blackwell, Oxford, pp. 173–200.

Ruszkiczay-Rüdiger, Z., Braucher, R., Csillag, G., Fodor, L.I., Dunai, T.J., Bada, G., Bourlés, D. & Müller, P., 2011: Dating Pleistocene aeolian landforms in Hungary, Central Europe, using in situ produced cosmogenic ^{10}Be. *Quaternary Geochronology* 6, 515–529.

Rybár, S., Kováč, M., Šarinová, K., Halásová, E., Hudáčková, N., Šujan, M., Kováčová, M., Ruman, A. & Klučiar, T., 2016: Neogene changes in Paleogeography, Paleoenvironment and the Provenance of sediment in the Northern Danube Basin. *Bulletin of Geosciences* 91, 367–398.

Sallenger, A.H., 1979: Inverse grading and hydraulic equivalence in grain-flow deposits. *Journal of Sedimentary Petrology* 49, 553–562.

Sanders, D., Ortner, H. & Pomella, H., 2018: Stratigraphy and deformation of Pleistocene talus in relation to a normal fault zone (central Apennines, Italy). *Sedimentary Geology* 373, 77–97.

Slootman, A. & Cartigny, M.J.B., 2020: Cyclic steps: Review and aggradation-based classification. *Earth-Science Reviews* 201, 102949.

Swan, F.H., 1988: Temporal clustering of paleoseismic events on the Oued Fodda fault, Algeria. *Geology* 16, 1092–1095.

Sztanó, O., Kováč, M., Magyar, I., Šujan, M., Fodor, L., Uhrin, A., Rybár, S., Csillag, G. & Tokés, L., 2016: Late Miocene sedimentary record of the Danube/Kisalföld Basin: Interregional correlation of depositional systems, stratigraphy and structural evolution. *Geologica Carpathica* 67, 525–542.

Sztanó, O., Magyar, I., Szónoky, M., Lantos, M., Müller, P., Lenkey, L., Katona, L. & Csillag, G., 2013: Tihany Formation in the surroundings of Lake Balaton: Type locality, depositional setting and stratigraphy. *Földtani Közlöny* 143, 1, 73–98 (in Hungarian with English abstract).

Šarinová, K. & Maglay, J., 2002: Sedimentology and petrography of Lukáčovce Mb. in the Nitrianska Pahorkatina Upland. *Slovak Geological Magazine* 8, 3–11.

Šujan, M., Braucher, R., Kováč, M., Bourlès, D.L., Rybár, S., Guillou, V. & Hudáčková, N., 2016: Application of the authigenic $^{10}Be/^{9}Be$ dating method to Late Miocene–Pliocene sequences in the northern Danube Basin (Pannonian Basin System): Confirmation of heterochronous evolution of sedimentary environments. *Global and Planetary Change* 137, 35–53.

Šujan, M., Braucher, R., Rybár, S., Maglay, J., Nagy, A., Fordinál, K., Šarinová, K., Sýkora, M., Józsa, Š. & Kováč, M., 2018: Revealing the late Pliocene to Middle Pleistocene alluvial archive in the confluence of the Western Carpathian and Eastern Alpine rivers: $^{26}Al/^{10}Be$ burial dating from the Danube Basin (Slovakia). *Sedimentary Geology* 377, 131–146.

Šujan, M., Kováč, M., Hók, J., Šujan, M., Braucher, R., Rybár, S. & de Leeuw, A., 2017: Late Miocene fluvial distributary system in the northern Danube Basin (Pannonian Basin System): Depositional processes, stratigraphic architecture and controlling factors of the Piešťany Member (Volkovce Formation). *Geological Quarterly* 61, 521–548.

Šujan, M., Rybár, S., Kováč, M., Bielik, M., Majcin, D., Minár, J., Plašienka, D., Nováková, P. & Kotulová, J., 2021: The polyphase rifting and inversion of the Danube Basin revised. *Global and Planetary Change* 196, 103375.

Utescher, T., Erdei, B., Hably, L. & Mosbrugger, V., 2017: Late Miocene vegetation of the Pannonian Basin. *Palaeogeography, Palaeoclimatology, Palaeoecology* 467, 131–148.

Valentin, C., Poesen, J., Li, Y., 2005: Gully erosion: Impacts, factors and control. *Catena* 63, 2-3, 132–153.

van Dam, J.A., 2006: Geographic and temporal patterns in the late Neogene (12-3 Ma) aridification of Europe: The use of small mammals as paleoprecipitation proxies. *Palaeogeography, Palaeoclimatology, Palaeoecology* 238, 190–218.

Vasiliev, I., de Leeuw, A., Filipescu, S., Krijgsman, W., Kuiper, K., Stoica, M. & Briceag, A., 2010: The age of the Sarmatian–Pannonian transition in the Transylvanian Basin (Central Paratethys). *Palaeogeography, Palaeoclimatology, Palaeoecology* 297, 54–69.

Vass, D., 2002: Litostratigrafia Západných Karpát: neogén a budínsky paleogén [EN: Lithostratigraphy of the Western Carpathians: Neogene and Buda Paleogene]. State Geological Survey of Dionýz Štúr, Bratislava.

Vass, D., Elečko, M. & Fordinál, K., 2002: Závada – Bielice Rise – a buried elevation between Bánovce and Rišňovce Depressions in the Danube Basin. *Slovak Geological Magazine* 8, 13–20.

Wagner, T., Fritz, H., Stüwe, K., Nestroy, O., Rodnight, H., Hellstrom, J. & Benischke, R., 2011: Correlations of cave levels, stream terraces and planation surfaces along the River Mur-Timing of landscape evolution along the eastern margin of the Alps. *Geomorphology* 134, 62–78.

Wang, Z., Meyer, M.C. & Hoffmann, D.L., 2016: Sedimentology, petrography and early diagenesis of a travertine–colluvium succession from Chusang (southern Tibet). *Sedimentary Geology* 342, 218–236.

Yawar, Z. & Schieber, J., 2017: On the origin of silt laminae in laminated shales. *Sedimentary Geology* 360, 22–34.

Supplementary Table 1: Coordinates of the studied outcrops.

Locality	Lon	Lat
Lúka-1	48.67322	17.88189
Lúka-2	48.67778	17.88273
Modrová-1	48.64726	17.88539
Modrová-2	48.64179	17.89518
Modrovka	48.65202	17.88911
Tesáre	48.61503	18.07290